

Attributing and Verifying European and National Greenhouse Gas and Aerosol Emissions and Reconciliation with Statistical Bottom-up Estimates

Deliverable 2.2 Anthropogenic emission inventories and natural flux data sets

Authors: R. Dröge, S. van Mil, I. Super, H.

Denier van der Gon, D. Brunner, L. Constantin, U.

Karstens, Z. Wu, F. Lagergren, M. Scholze, M. Lundblad, H.

Witt, M. van Zanten

Date: 02-07-2024

Dissemination: Public/Restricted

Work package: 2.1 Version: 1.0



This project has received funding from the European Union's Horizon Europe research and innovation programme under grant agreement No. 101081322

Views and opinions expressed are however those of the author(s) only and do not necessarily reflect those of the European Union or the Climate, Infrastructure and Environment Executive Agency (CINEA). Neither the European Union nor the granting authority can be held responsible for them.

Attributing and Verifying European and National Greenhouse Gas and Aerosol Emissions and Reconciliation with Statistical Bottom-up Estimates (AVENGERS)

Call: HORIZON-CL5-2022-D1-02

Topic: HORIZON-CL5-2022-D1-02-01

Type of action: HORIZON Research and Innovation Actions

Granting authority: European Climate, Infrastructure and Environment Executive Agency

Project starting date: 01/01/2023

Project end date: 30/06/2026

Project duration: 42 months

Contact: Dr. Marko Scholze, Coordinator

Lund University, Sweden

Document history:

Version	Author(s)	Date	Changes
0.1	R. Dröge (TNO), S. van Mil (TNO), I.	17-06-2024	-
	Super (TNO), H. Denier van der Gon (TNO), D. Brunner (EMPA), L.		
	Constantin (EMPA), U. Karstens		
	(ULUND), Z. Wu (ULUND), F.		
	Lagergren (ULUND), M. Scholze		
	(ULUND), M. Lundblad (SLU), H.		
	Witt (RIVM), M. van Zanten (RIVM)		
1.0	R. Dröge (TNO)	02-07-2024	Review comments processed

Internal review:

Sander Houweling (VUA), 30-06-2024

Table of Contents

1 DELIVERABLE OBJECTIVES	4
2 INTRODUCTION	5
2.1 Anthropogenic emissions	6
3 ANTHROPOGENIC FLUXES	9
3.1 METHODOLOGY	
4 NATURAL FLUXES	19
4.1 METHODOLOGY 4.1.1 CO ₂ simulations 4.1.2 CH ₄ simulations 4.1.3 N ₂ O simulations 4.2 RESULTS 4.2.1 CO ₂ 4.2.2 CH ₄ 4.2.3 N ₂ O	
5 TEMPORAL AND VERTICAL PROFILES OF ANTHROPOGENIC FLUXES	28
5.1 Temporal profiles $5.1.1$ CO_2 $5.1.2$ CH_4 $5.1.3$ N_2O 5.2 Vertical profiles.	
6 PRIOR UNCERTAINTIES OF ANTHROPOGENIC FLUXES	32
6.1 Methodology	
REFERENCES	36
ANNEX 1 TEMPORAL PROFILES	40
ANNEX 2 FIRST COMPARISON FOR ANTHROPOGENIC N2O TO EDGARV8	42

1 Deliverable objectives

The objective of deliverable 2.2 Data set on anthropogenic emissions and natural fluxes for European inversion and national case studies is to provide a complete data set of prior emissions from anthropogenic and natural sources. These emissions will be used in tasks 2.3, 2.4 and 2.5 to calculate European top-down estimates of anthropogenic and natural CO_2 , CH_4 and N_2O fluxes, and in task 2.6 for the national case studies.

2 Introduction

This report provides an overview of the data available for the anthropogenic and natural priors. This includes anthropogenic fluxes (section 3), natural fluxes (section 4), temporal and vertical profiles (section 5) and prior uncertainties (section 6).

Data is available on the Avengers Sharepoint for internal use within this project. The national inventory agencies indicated that part of the national gridded emission inventories cannot be made publicly available, therefore the data will only be shared with the Avengers project partners.

The available datasets consist of Anthropogenic emissions and accompanying emission characteristics and natural emissions.

2.1 Anthropogenic emissions

Available datasets for anthropogenic emissions:

- Spatial gridded emissions
 - TNO-GHGco_v7: Anthropogenic emissions, as prepared by TNO. This consists of a csv and netcdf file for each year with the year total emissions of CO₂, CH₄ and N₂O per 0.1° x 0.05° gridcell and per GNFR category (kg/gridcell/year).
 - TNO-GHGco_v7_Avengers_countries: Anthropogenic emissions, as prepared by TNO but the gridded data from Germany, Italy, the Netherlands, Sweden and Switzerland are replaced by the official gridded data as prepared by the respective national inventory agencies. This consists of a csv and netcdf file for each year with the year total emissions of CO₂, CH₄ and N₂O per 0.1° x 0.05° gridcell and per GNFR category (kg/gridcell/year)
- Temporal profiles
 - AVENGERS_time_monthly: Time profile for anthropogenic emissions for month per year. This consist of a csv file for each gas separately, with a time profile per GNFR category and per country.
 - AVENGERS_time_weekly: Time profile for anthropogenic emissions for day per week.
 This consist of a csv file for each gas separately, with a time profile per GNFR category and per country.
 - AVENGERS_time_daily: Time profile for anthropogenic emission for hour per day.
 This consist of a csv file for each gas separately, with a time profile per GNFR category and per country.
 - AVENGERS_time_daily_per_year: Time profile for anthropogenic emissions for day per year (for the sectors other stationary combustion and solid waste disposal). This consists of a csv file for CO₂ and CH₄ separately, with a time profile per country (stationary combustion) or per 1° x 1° gridcell (solid waste disposal).
- Vertical profiles
 - AVENGERS_vertical: Vertical profile for anthropogenic emissions. This consist of an excel file for each gas separately, with a vertical profile in 7 height classes per GNFR category.
- Uncertainties
 - AVENGERS_GHGs_year2021_uncertainties: Uncertainty and spatial error correlation length. This consist of a netcdf file for the uncertainty of all gases, with uncertainties and spatial error correlation per GNFR category and per country.

2.2 Natural emissions

Available datasets for natural emissions:

CO₂:

- o Conv_lpj_hgpp_eu_0.5deg: Gross primary production as modelled with LPJ Guess. This consist of a netcdf file for each year with the hourly CO_2 emission at 0.5° x 0.5° (μ mol/m²/sec). The data is available via the <u>ICOS Carbon portal</u>.
- Conv_lpj_hrtot_eu_0.5deg: Total respiration as modelled with LPJ Guess. This consist
 of a netcdf file for each year with the hourly CO₂ emission at 0.5° x 0.5°
 (μmol/m²/sec). The data is available via the ICOS Carbon portal.
- Onv_lpj_hnee_eu_0.5deg: Net ecosystem exchange as modelled with LPJ Guess. This equals gross primary production plus total respiration. This consist of a netcdf file for each year with the hourly CO_2 emission at 0.5° x 0.5° (μ mol/m²/sec). The data is available via the ICOS Carbon portal.

CH₄:

- o cal_lpj_ch4_net_peat: Net emissions from peatlands. This consist of a netcdf file for each year with the daily CH₄ emission at 0.5° x 0.5° (mg CH₄/m²/day).
- o cal_lpj_ch4_net_inun: Net emissions from inundated wetlands. This consist of a netcdf file for each year with the daily CH₄ emission at 0.5° x 0.5° (mg CH₄/m²/day).
- o cal_lpj_ch4_emi_mineral: Emissions from mineral soils. This consist of a netcdf file for each year with the daily CH₄ emission at 0.5° x 0.5° (mg CH₄/m²/day).
- o cal_lpj_ch4_uptake_mineral: Update in mineral soils. This consist of a netcdf file for each year with the daily CH₄ uptake at 0.5° x 0.5° (mg CH₄/m²/day).

N₂O:

- o dnflux_crop: Flux of nitrogen components in croplands. This consist of a netcdf file for all years together with the daily N_2O emission at 0.5° x 0.5° (kg N/ha/day). Also NH₃, NO_x and N₂ is included in this file.
- o dnflux_nat: Flux of nitrogen components in natural areas. This consist of a netcdf file for all years together with the daily N_2O emission at 0.5° x 0.5° (kg N/ha/day). Also NH₃, NO_x and N₂ is included in this file.
- o dnflux_past: Flux of nitrogen components in pastures. This consist of a netcdf file for all years together with the daily N_2O emission at 0.5° x 0.5° (kg N/ha/day). Also NH₃, NO_x and N₂ is included in this file.
- dnflux_tot: Flux of nitrogen components in croplands, natural areas and pastures.
 This consist of a netcdf file for all years together with the daily N₂O emission at 0.5° x 0.5° (kg N/ha/day). Also NH₃, NO_x and N₂ is included in this file.

2.3 Additional information on the datasets

For several sectors, there is (partial) double counting in the datasets of the anthropogenic emissions and the natural emissions. An overview of anthropogenic source sectors is provided in Table 1, and a description of the natural emissions is provided in section 4. To ensure that no double counting occurs in the modelling, the following choices can be made.

For CO₂, there is an overlap in the emission files between:

- CO₂ emissions from carbon stock change (category Qc in the anthropogenic dataset). This includes fluxes due to primary production, respiration and also disturbances like harvesting.
- CO₂ from biomass combustion (categories Ab, Bb, Cb, Fb, Gb, Hb, Ib, Jb and Lb in the anthropogenic dataset). This includes emissions from solid, liquid and gaseous biomass combustion, and also includes emissions from the biogenic part of waste combustion.
- CO₂ emissions from Net Ecosystem Exchange (category NEE in the natural dataset). This
 includes fluxes from gross primary production, autotrophic and heterotrophic respiration
 It is advised to use the CO₂ emissions from CO₂ from biomass combustion (categories Ab, Bb, Cb, Fb,
 Gb, Hb, Ib, Jb and Lb in the anthropogenic dataset) and CO₂ emissions from Net Ecosystem Exchange
 (category NEE in the natural dataset). To avoid double counting, the CO₂ emissions from carbon stock
 change (category Qc in the anthropogenic dataset) should be excluded.

For N₂O, there is an overlap in the emission files between:

- Direct N₂O emissions from agriculture and LULUCF (categories Kf, Lf, Lb, Qnm and Qni in the anthropogenic dataset). This includes N₂O emissions from manure application in agriculture and in managed forests.
- Indirect N₂O emissions from agriculture and LULUCF from atmospheric deposition (categories Kid, Lid and Qi in the anthropogenic dataset). The N₂O is emitted after atmospheric deposition of NH₃ from anthropogenic sources (NH₃ from agriculture and LULUCF).
- N₂O fluxes from croplands, pastures and natural areas, as calculated by LPJ Guess (categories Nflux_crop, Nflux_past and Nflux_nat in the natural dataset). LPJ Guess uses atmospheric deposition, biological nitrogen fixation (BNF) and fertilisation as input data.

It is advised to use direct N_2O emissions from agriculture and LULUCF (categories Kf, Lf, Lb, Qnm and Qni in the anthropogenic dataset), indirect N_2O emissions from agriculture and LULUCF (categories Kid and Lid in the anthropogenic dataset) and N_2O fluxes from natural areas in the natural dataset. To avoid double counting, N_2O fluxes from croplands and pastures in the natural dataset should be excluded.

Indirect N_2O emissions (caused by reemissions after atmospheric deposition of NH_3) are partly considered in both the anthropogenic inventory of TNO (category Kid, Lid and Qi in the anthropogenic dataset) and in the simulations with LPJ-GUESS, as nitrogen deposition is one of the input parameters in the LPJ Guess model. This is a partial overlap, which makes it impossible to completely avoid double counting. If the anthropogenic indirect emissions would be excluded, then the indirect N_2O emissions from other land than natural areas would be excluded as well. And if the natural N_2O emissions would be excluded, then the N_2O fluxes due to biological nitrogen fixation would be excluded as well. Therefore, it is advised to use both datasets, even though there is some double counting in the two datasets.

The dataset with anthropogenic emission contains indirect emissions from N-deposition due to agricultural activities (mainly NH_3 deposition and leaching), but N-deposition due to non-agricultural sources is not considered. To fill this gap, David Simpson from Met.Norway is running additional simulations with the EMEP model to compute deposition fluxes of reduced and oxidized N due to non-agricultural sources. This datasource could be used additionally to complete the indirect N_2O emissions in Europe. This dataset will be prepared later and is not part of this deliverable.

For fire emissions (CO_2 , CH_4 and N_2O), there is an overlap in the emission files between:

- Biomass combustion in the LULUCF sector (category Qb in the anthropogenic dataset). This includes emissions from wildfires and intentional fires
- Fire emissions in the natural datasets for CO₂ and N₂O. This only includes wildfires and the emissions are stochastically determined

For N_2O , the natural emission fluxes from fires are included separately in the LPJ Guess output. The order of magnitude of the fire emissions in Europe in the anthropogenic dataset and the natural dataset is the same, but there are large differences for individual countries. For CO_2 , these emissions are not separately included in the LPJ Guess output, as this is part of the model itself. For CH_4 , no fire emissions are included in LPJ Guess.

It is advised to use the emissions from LULUCF (category Qb in the anthropogenic dataset) for all three gases, as this includes both wildfires and intentional fires. This does result in a (partial) double counting with the CO_2 emissions from wildfires in the natural dataset, as these cannot be excluded. To avoid double counting, N_2O emissions from fires in the natural dataset should be excluded.

3 Anthropogenic fluxes

Gridded anthropogenic emissions for CO_2 , CH_4 and N_2O are provided at about 6x6 km resolution (0.1 x 0.05°) for the years 2010-2021, based on officially reported country-level emissions. For CO_2 and CH_4 , this has been built upon previous work in the EU projects VERIFY and CoCO2 (see Denier van der Gon, et al., 2023), while for N_2O , the gridding routine has been updated following a similar method as CO_2 and CH_4 . For the case studies (Germany, Italy, the Netherlands, Sweden and Switzerland), additional national gridded inventories have been provided by the GHG inventory experts of the National Agencies in the project, which make use of more detailed and/or different geo-statistical data available in the country. A comparison between the European emission inventory and the national gridded inventories have been made to identify the main differences and to learn lessons on shortcomings or uncertainties in the inventories.

The gridded anthropogenic fluxes are available in csv and netcdf format, and contain the following data:

- Species: CO₂, CH₄, N₂O
- Years: 2010-2021 (annual emissions for 12 individual years)
- Countries: Europe (30°W-60°E, 30°N-72°N)
- Sector aggregation: GNFR categories (A to Q), with an additional split for fossil/biogenic
 emissions, an additional split for direct and indirect emissions and an additional split for
 landfills and waste water treatment plants. Furthermore, emissions of LULUCF are included
 (with a new GNFR category Q_LULUCF). See Table 1 for details. This split is only included for
 the European countries. For the other countries, no additional split is included.
- Spatial resolution: 0.1° x 0.05° (lon-lat)
- Data type: Point sources and area sources are defined separately. Point sources include specific coordinates of that point, while area sources include coordinates of the middle of the grid cell.
- Emission unit: kg per gridcell per year

3.1 Methodology

Two separate gridded anthropogenic emission inventories have been prepared:

- TNO-GHGco_v7: Emission inventory for all European countries.
- TNO-GHGco_v7_Avengers_countries: National gridded inventories from Germany, Italy, the Netherlands, Sweden and Switzerland, nested within the TNO-GHGco_v7 inventory for the other European countries.

The emissions in both datasets are based on the emissions submitted by countries to UNFCCC in 2023 (for years 1990-2021).

This section provides a description of the methodology for the TNO-GHGco_v7 inventory (section 3.1.1), the national gridded inventories of Germany, Italy, the Netherlands, Sweden and Switzerland (section 3.1.2) and the combination of the TNO inventory and the country inventories to prepare the TNO-GHGco_v7_Avengers_countries dataset (section 3.1.3).

Table 1 Source categories included in the emission inventories

GNFR Category	GNFR Category Parent	GNFR Category Name	
Ab	Α	A_PublicPower_biofuel	
Af	Α	A_PublicPower_fossil_fuel	
Bb	В	B_Industry_biofuel	
Bf	В	B_Industry_fossil_fuel	
Cb	С	C_OtherStationaryComb_biofuel	
Cf	С	C_OtherStationaryComb_fossil_fuel	
D	D	D_Fugitives	
Е	E	E_Solvents	
Fb	F	F_RoadTransport_Exhaust_biofuel	
Ff	F	F_RoadTransport_Exhaust_fossil_fuel	
Gb	G	G_Shipping_biofuel	
Gf	G	G_Shipping_fossil_fuel	
Hb	Н	H_Aviation_biofuel	
Hf	Н	H_Aviation_fossil_fuel	
Ib	1	I_OffRoad_biofuel	
If	1	I_OffRoad_fossil_fuel	
Jb	J	J_Waste_biogenic	
Jf	J	J_Waste_non-biogenic	
Jww	J	J_Waste_waste_water_treatment_plants	
Js	J	J_Waste_waste_solid_waste_disposal	
Kf	K	K_AgriLivestock_direct	
Kil	K	K_AgriLivestock_indirect_leaching_runoff	
Kid	K	K_AgriLivestock_indirect_atmospheric_deposition	
Lb	L	L_AgriOther_AGW	
Lf	L	L_AgriOther_other	
Lil	L	L_AgriOther_indirect_leaching_runoff	
Lid	L	L_AgriOther_indirect_atmospheric_deposition	
Qb	Q	Q_LULUCF_Biomass_burning	
Qc	Q	Q_LULUCF_Carbon_stock_change	
Qd	Q	Q_LULUCF_Drainage_and_rewetting	
Qi	Q	Q_LULUCF_indirect	
Qni	Q	Q_LULUCF_N_inputs	
Qnm	Q	Q_LULUCF_N_mineralization	
M	M	M_Other *	

^{*} M_Other is only included for country data for Switzerland.

3.1.1 TNO-GHGco inventory

For the TNO-GHGco_v7 emission inventory, the approach is similar to the CAMS-REG_v4 (as described in Kuenen et al., 2022) and to the TNO-GHGco_v5 (as described in Denier van der Gon et al., 2023) inventories. For CO₂ and CH₄, the inventory has been built upon previous work in the EU projects VERIFY and CoCO₂ (see Denier van der Gon, et al., 2023), while for N₂O, the gridding routine has been updated following a similar method as the gridding routine for CO₂ and CH₄.

In general, the spatially distributed emissions are based on national reported emissions per sector (from the 2023 submission to UNFCCC), which are spatially distributed based on specific proxies per sector, pollutant and year. For specific sources, an emission calculation has been added to replace

the emissions from the UNFCCC reporting, for example for agricultural waste burning, international shipping and CO_2 from aviation. Improvements implemented in this version of the gridded emission inventory, compared to the emission inventory from D2.2 in the CoCO2 project (Denier van der Gon et al., 2023), are:

- Base emission data for all sectors have been updated to the 2023 reporting to UNFCCC for the years 2010-2021.
- The spatial distribution for road transport emissions has been improved based on a new model
 of the road network and intensities, which has recently been completed in the framework of
 the Horizon2020 project Ri-URBANS. This has resulted in higher emissions in urban areas,
 compensated by lower emissions in other regions, bringing the emissions allocated to urban
 areas more in line with other estimates of traffic emissions in cities or urban areas.
- N₂O emissions are added to the gridded emission inventory. Proxies are similar to the proxies used for CH₄ and CO₂, with an exception for indirect emissions from agriculture. For indirect N₂O emissions through leaching and run-off (GNFR category Kil and Lil), modelled N₂O emissions at a 0.5° x 0.5° resolution by Wang et al. (2023) have been used as a proxy to spatially distribute emissions within a country. For indirect N₂O emissions through atmospheric deposition, modelled NH₃ deposition (with LOTOS-EUROS v2.3.000 with emissions from CAMS REG 6.1 for the year 2019 at 0.4° x 0.2° degree resolution) has been used as a proxy to spatially distribute emissions within a country. Additionally, the bottom-up calculation for agricultural waste burning (as described in Kuenen, et al., 2022) has been extended for N₂O.
- LULUCF emissions have been included for the first time. These emissions have been spatially gridded based on the land cover in the CORINE Land Cover dataset.
- GNFR categories are extended with an additional split for fossil/biogenic emissions, an
 additional split for direct and indirect emissions and an additional split for landfills and waste
 water treatment plants. See Table 1 for details. This split is only included for the European
 countries. For the other countries, no additional split is included.

3.1.2 National gridded inventories

Germany

The German Environment Agency (Umweltbundesamt, UBA) is responsible for the national, central database for emissions calculation and reporting in accordance with the UNFCCC - Kyoto protocol and UNECE-CLRTAP — Gothenburg protocol. Emissions from the agriculture and LULUCF sectors are recorded by the Thünen Institut and provided to the UBA inventory. The national emissions are calculated on a yearly basis, with a time series from 1990 to two years before the reporting year. Emissions are calculated as the product of activity rates and emission factors for the respective sectors and fuel types. To provide gridded emission data of air pollutants and greenhouse gases UBA developed the Gridding Emission Tool for ArcGIS (Greta). Greta uses the official inventory data to provide datasets for the AVENGERS project to assist the modelling activities in WP2.

Greta contains a complete set of the required data per base year. This includes emissions, distribution parameters, geometric datasets as well as the necessary definitions and allocation tables. For each NFR sector, the spatial distribution of the national emissions is determined using distribution parameters, and if possible, as point sources (PQ) and line sources (LQ). The remaining emissions are spatially assigned to distribution parameters on district level and further, considering land cover data, on area level (FQ). Furthermore, Greta considers the vertical distribution of

emissions, including those from aviation, power plants or industry, which are e.g. stack heights or landing and take-off cones at airports.

The maximum spatial resolution of the national gridded emission that can be obtained from GRETA is 1x1 km². The emissions of all parts of a geometry (PQ/LQ/FQ) covered by a grid cell are attributed to the respective raster cell. This process results in the production of a raster with high spatial and thematic resolution, as well as different nomenclatures for reporting: (NFR, GNFR, SNAP). The data can be exported in the form of a GIS data, csv files, or as standard NetCDF format.

Recent Research (Dammers et al. 2022) showed that there is a very close structural similarity between short lived air pollutants (NO_x) detected by TROPOMI and emissions computed by GRETA of up to 79%. This comparison of the spatial structure of the gridded inventory data with the actual spaceborne data from TROPOMI validates the GRETA approach for NO_x and may potentially suggest its robustness for other co-emitted species from combustion processes.

Further information on Germany's gridding procedure can be obtained via:

https://iir.umweltbundesamt.de/2024/general/gridded_data/start

Italy

The Italian Inventory Agency ISPRA produced distributed emissions at province level (NUTS3) every five years, increasing to every four years from 2017. For the years 2010 – 2015 – 2019, the most updated estimates has been developed in 2021 and a report (in Italian) containing the detailed description of the methodology used is available here:

https://www.isprambiente.gov.it/en/publications/reports/the-disaggreagation-at-the-provincial-level-of-the-national-inventory-of-emissions?set language=en

The breakdown for all the provinces of the Italian territory for each source category was carried out through the use of proxies derived from the processing of a database of over 1 million and 600 thousand records of statistical data of various kinds: demographic, economic, industrial production indicators (such as population, vehicle registration, air traffic, consumption of products, consumption of fuels, etc.) and other territorial ones relating to land use (for example agricultural land, covered by forests or vegetation, etc.).

Emissions per province and per source sector were then equally distributed on EMEP grid 0.1° x 0.1° , and then rescaled on the 0.1° x 0.05° grid.

Point sources with known locations were reported in addition to these gridded emissions: thermoelectric power plants, large industries, incinerators and landfills; data were collected from national registries Emissions Trading, E-PRTR (European Pollutant Release and Transfer Register) and LCP (Large Combustion Plants), as well as from authorization procedures (IPPC, AIA, VIA), EMS (Emissions Monitoring Systems), Plants' Inspections Reports.

For the intermediate years in the interval 2010-2021, where no spatially distributed emission were available, the spatial distribution of the closest available year was used (hereafter called *reference years*). Specifically, for 2011 and 2012 the spatial distribution from 2010 was used, for 2013, 2014, 2016, 2017 the spatial distribution from 2015 was used, and for 2018, 2020, 2021 the spatial distribution of 2019 was used. For missing years the emissions per grid cell were calculated as the product of the national emissions for each GNFR category source (CRF submission 2023) and the percentage contribution of that cell in the reference years and concerning category source (including point sources).

As gridded emissions 2010, 2015 and 2019 were derived from CRF submission 2021, in order to improve consistency, also for these three reference years CFR submission 2023 were used and scaled to grid cells equally as done for intermediate missing years.

Contributors from ISPRA: Angela Fiore, Eleonora Di Cristofaro, Ernesto Taurino

The Netherlands

In general, the Dutch national inventory produces every year spatially distributed emissions for a selection of years, currently for 2010, 2015, 2019, 2020, and 2021. For these years, gridded emissions were produced by distributing the total national emissions based on suitable proxies for their localization on a 0.1 x 0.05° grid. A detailed overview over the used proxies is available under https://www.emissieregistratie.nl/documentatie/ruimtelijke-verdeling (in Dutch). When no spatial proxy was available, as was only the case for LULUCF emissions, emissions were evenly distributed over the entire Netherlands. Large point sources with known locations were reported in addition to these gridded emissions.

For the intermediate years, where no spatially distributed emission are available, the spatial distribution of the closest available year was used. Specifically, for 2011 and 2012 the spatial distribution from 2010 was used, for 2013, 2014 and 2016 the spatial distribution from 2015 was used, and for 2017 and 2018 the spatial distribution of 2019 was used. To that end, spatially distributed emission maps for the reference year were produced on the level of individual emission sources. The emission per grid cell were then scaled by the change in total emissions for this emission source compared to the target year. These interpolated results were then verified against the total national emissions of the target year.

Contributors from RIVM: Margreet van Zanten, Hannes Witt, Romuald te Molder, Guido Hollman, Loes van der Net

Sweden

The gridded data for Sweden originates from the national emission database (https://nationellaemissionsdatabasen.smhi.se) which presents Sweden's national total emissions of emissions to air for 29 substances distributed at county and municipal level. The emissions are presented for 54 different sectors divided into nine main sectors. The database builds on the reporting requirements under the United Nations Framework Convention on Climate Change (UNFCCC) and the Convention on Long-Range Transboundary Air Pollution (CLRTAP) for greenhouse gases and other air pollutants. It covers emissions both from diffuse sources, such as road traffic, and from point sources such as industrial facilities. A method and quality description for geographically distributed emissions for the years 1990, 2000, 2005, 2010, and 2015-2022 is available in Swedish (Englund et. al. 2024).

The geographical distribution is mainly carried out according to a "top-down" concept. This means that emissions are broken down from a national total emission to the county and municipality level and further to a grid with a resolution of 1 km². The distribution takes place with the help of relevant statistics and geographical data, for example the location of industries, road networks, grazing land, and population data. The results for all sectors are presented with the same geographical resolution, although the quality varies. A quality description using quality grading can provide guidance on the uncertainties that exist at the main sector level.

To provide gridded data for the AVENGERS project the gridded inventory described above was aggregated to the $0.1 \times 0.05^{\circ}$ grid and the years with no gridded data (i.e. 2011-2014) was interpolated and scaled using the total emissions per sector and gas.

No gridded data is currently available for the biogenic emissions of CO₂ or the LULUCF emissions.

Contributors from SLU: Mattias Lundblad

Switzerland

The gridded Swiss inventory is based on officially reported total annual emissions and on source-specific rasters for the year 2015. Thus, while total emissions change from year to year, the spatial allocation per category remains constant.

Total emissions of anthropogenic categories correspond to the numbers officially reported by Switzerland to UNFCCC¹⁾. These are generated by the Swiss Federal Office for the Environment (FOEN) using the Swiss emission information system EMIS²⁾. EMIS combines a comprehensive database of statistical data and emission factors with tools to produce Switzerland's official inventory reports for various international conventions including the Paris Agreement.

The emissions for the years 2011-2021 are based on the national inventory report (NIR) of 2023. For 2022, data from the most recent NIR of 2024 is used. The spatial mapping of individual source categories is based on rasters at 100 m x 100 m resolution provided by the company Meteotest for 52 individual source categories.

Projection from these high-resolution rasters to the common grid of 0.1° x 0.05° used in AVENGERS is accomplished with Empa's python package emiproc https://emiproc.readthedocs.io/. The tool also aggregates the 52 original source categories to the 14 GNFR categories used in AVENGERS. Emissions from big industrial facilities (point sources) are reported separately at their exact locations. The remaining emissions are reported as area emissions on the 0.1°x 0.05° grid.

Gridded data for LULCUCF categories are not yet available but are expected to become available in the course of 2024, earliest in June 2024.

Weblinks:

¹⁾ Swiss National Emission Inventory: https://www.bafu.admin.ch/bafu/en/home/topics/climate/state/data/climate-reporting/ghg-inventories.html

²⁾ Emission Information System EMIS: https://www.bafu.admin.ch/bafu/de/home/themen/luft/zustand/emissionsinformationssystem-der-schweiz-emis.html

Contributors from Empa are: Dominik Brunner, Lionel Constantin, Corina Keller

3.1.3 Combining country gridded inventories with TNO GHG inventory

The TNO-GHGco_v7_Avengers_countries consist of a combination of the TNO-GHGco_v7 inventory and the country gridded inventories of Germany, Italy, the Netherlands, Sweden and Switzerland. For nesting the country gridded inventories within the TNO inventory, some actions have been taken to maintain consistency between countries, as described in the following paragraphs.

The TNO-GHGco_v7 inventory contains both point sources and area sources. The German and Swedish gridded inventories do not contain the same distinction between point sources and area sources, but instead, these emissions are implemented in the grid and labelled as area sources. For the vertical profiles, it is important to distinguish between area and point sources, as point sources emit in general at higher altitude (see section 5.2). Therefore, to approximate the most realistic situation, when there is no distinction between area sources and point sources, it is assumed that all emissions in GNFR A and B are point sources, and that all emissions in other GNFR categories are area sources.

The TNO-GHGco_v7 inventory contains LULUCF emissions for all countries. The German, Swedish and Swiss gridded inventories do not include LULUCF emissions. For consistency, we have added the LULUCF emissions from the TNO-GHGco_v7 inventory for these countries in the TNO-GHGco_v7_Avengers_countries inventory.

The TNO-GHGco_v6 inventory contain emissions from sea shipping. The Netherlands has also provided emissions from P_Int_Shipping near the Dutch coast. As there is (partially) double counting with the (international) seashipping from TNO, these Dutch emissions from P_Int_Shipping have not been included in the TNO-GHGco_v7_Avengers_countries inventory.

The TNO-GHGco_v6 inventory distinguish between fossil and biogenic emissions. The German and Swedish inventory did not contain a distinction between fossil and biogenic emissions. Biogenic CO_2 emissions are missing from these inventories. Biogenic CH_4 and N_2O emissions are included as fossil CH_4 and N_2O emissions.

The Netherlands report natural emissions (included in N_Natural). As there is likely an overlap with the natural emissions from LPJ-Guess (see section 4), these emissions have not been included in the TNO-GHGco_v7_Avengers_countries inventory.

Overall, the country reported emissions include the same GNFR sector categories as the TNO-GHGco_v7 Inventory. However, for some GNFR categories, there is a difference in the level of detail included in the country inventories and the TNO-GHGco_v7 inventory. These differences in categories are included in the TNO-GHGco_v7_Avengers_countries inventory as provided by the countries and in the TNO-GHGco_v7 inventory, without any changes:

- For the waste sector (GNFR J), country reported data only distinguished between Jb (biogenic) and Jf (other), whereas the TNO-GHGco_v7 inventory also includes more detailed sectors Jww (waste water treatment plants) and Js (solid waste disposal).
- For the indirect N₂O emissions from agriculture, country reported data only distinguish between Ki and Li, whereas in the TNO-GHGco_v7 inventory we also distinguish between indirect emissions from atmospheric deposition (Kid and Lid), and leaching and runoff (Kil and Lil).
- The sector M_Other (GNFR M) is only included in the Swiss inventory. Other countries have no emissions in 'Other' sectors.

3.2 Results

The datasets of anthropogenic emissions contain emissions per country, GNFR sector and 0.1x0.05 degree grid cell. The data is available for the years 2010-2021. Figure 1 shows the trend in emissions between 2010 and 2021 for the EU27+ (EU, Norway, Iceland, Switzerland and United Kingdom). For CO₂, the main emission sources are power production (GNFR A), industry (GNFR B), other stationary combustion (GNFR C) and road transport (GNFR F). Other sectors have only a small contribution to the CO₂ emissions of European countries. For CH₄, the main emissions occur from agriculture

livestock (GNFR K), waste (GNFR J) and fugitives (GNFR D), while for N_2O the main share in emissions is caused by agriculture other (GNFR L). For CO_2 emissions, the impact of the covid pandemic in 2020 is clearly visible while CH_4 and N_2O emissions were not affected.

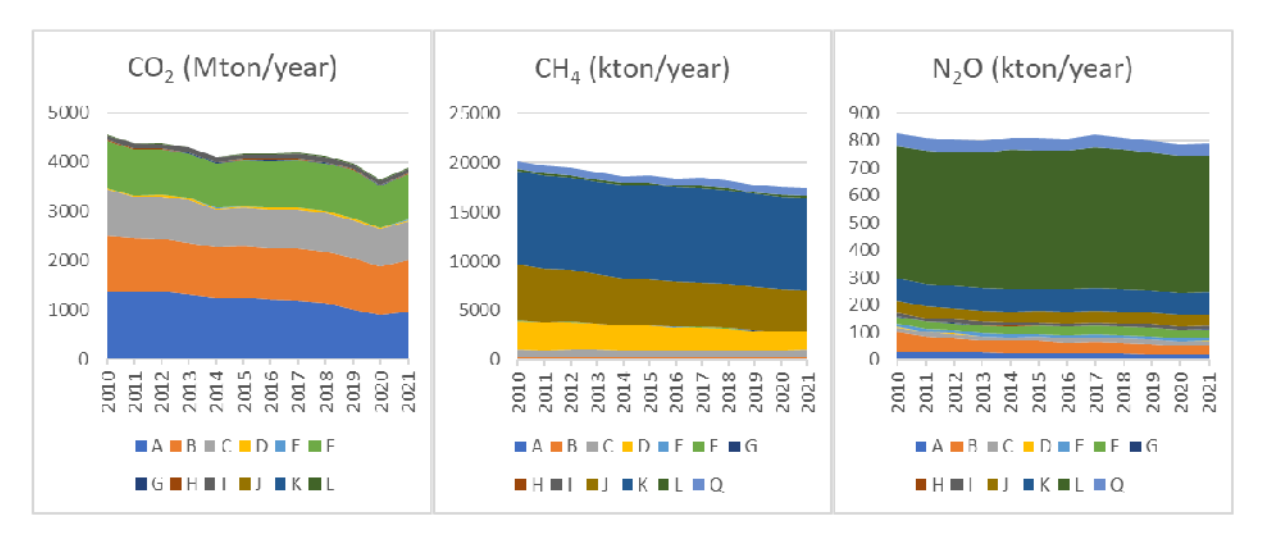


Figure 1: Trends for CO₂, CH₄ and N₂O emissions in the EU27+ (EU, and Norway, Iceland, Switzerland and United Kingdom) per GNFR category

Figure 2 shows a comparison between the TNO-GHGco_v7 emission inventory for the 5 case study countries and the gridded emissions provided by the country themselves. The emissions have been scaled for comparison. The country gridded emissions are set at 100% and the TNO gridded emissions are scaled to these country gridded emissions. The main difference is visible for CO₂ emissions from Sweden and Germany. This is caused by the fact that no biogenic CO₂ emissions are included in the country gridded emissions. The other differences are small, and they are partly due to some changes in the TNO-GHGco_v7 dataset, compared to the reported UNFCCC emissions. Within the TNO inventory, the emissions from international shipping, aviation and agricultural waste burning are estimated separately, instead of using the country reported data. Furthermore, there could be some small differences in allocation to the several GNFR categories.



Figure 2: Comparison between emissions in the TNO-GHGco_v7 inventory and in the gridded country emissions for 2021. The country data has been set to 100%, and the TNO-GHGco_v7 data has been scaled to the country data.

Figure 3 shows the spatial distribution of the total CO_2 , CH_4 and N_2O emissions in Europe, as included in the TNO-GHGco_v7_Avengers_countries dataset and the TNO-GHGco_v7 dataset. Main emission sources of CO_2 are located near cities, roads and industrial areas, while the main emission sources of CH_4 and N_2O are located in agricultural areas.

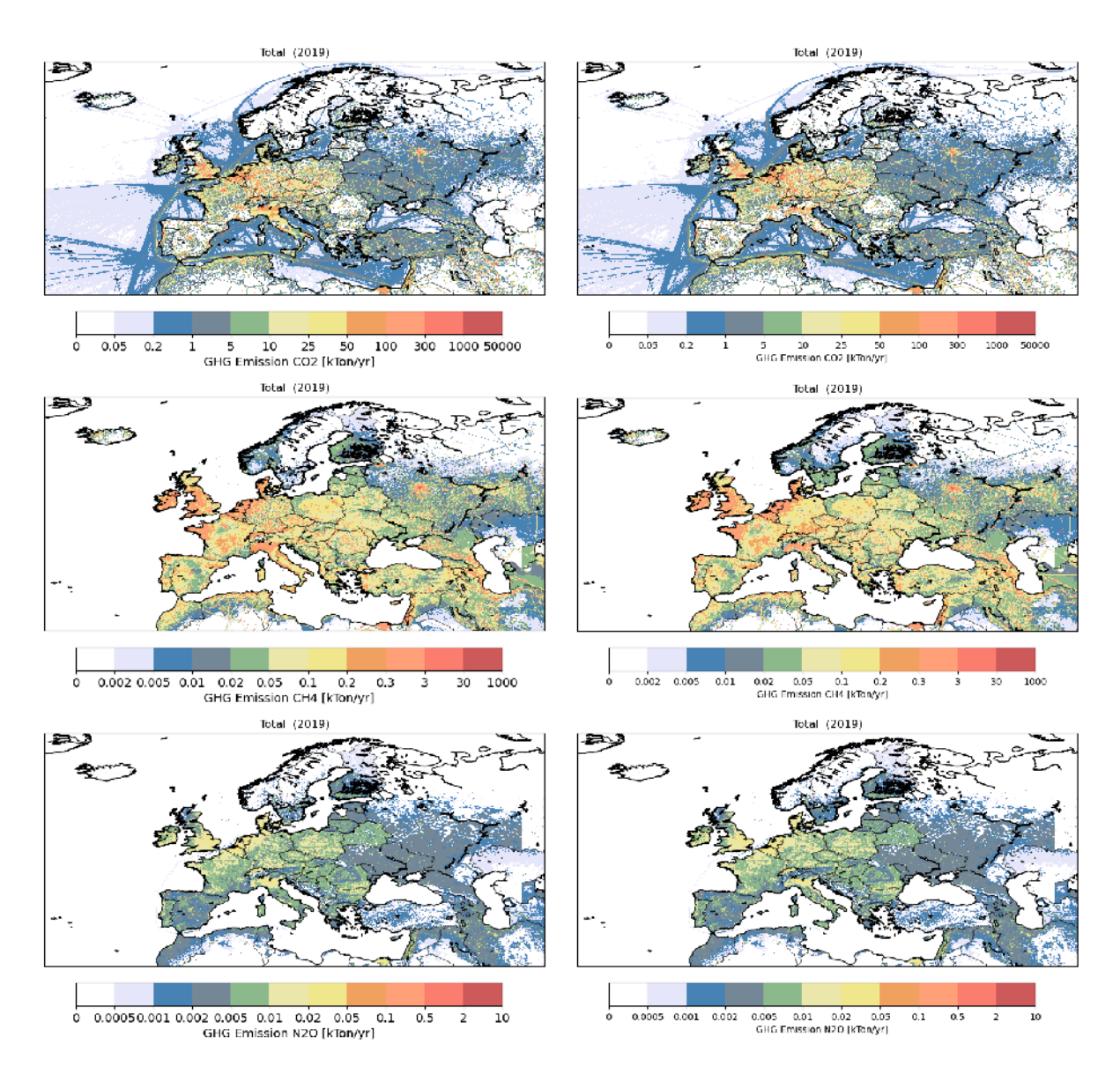


Figure 3: Gridded emissions in 2019 for CO₂, CH₄ and N₂O, as included in the TNO-GHGco_v7_Avengers_countries dataset (left) and the TNO-GHGco_v7 dataset (right)

4 Natural fluxes

Gridded natural surface atmosphere exchange fluxes for CO_2 , CH_4 and N_2O over Europe (Latitude: $35^\circ N-71^\circ N$, Longitude: $10^\circ W-35N^\circ$) are provided at $0.5^\circ \times 0.5^\circ$ spatial and either hourly in the case of CO_2 or daily in the case of CH_4 and N_2O temporal resolution covering the years 2010 to 2022 (in the case of N_2O to 2020). The fluxes have been calculated by employing the dynamic global vegetation model LPJ-GUESS (Smith et al., 2001), which is explained in more detail in section Methodology4.1.

4.1 Methodology

LPJ-GUESS (Lund-Potsdam-Jena General Ecosystem Simulator) is a process-based dynamic vegetation-terrestrial ecosystem community model designed for regional or global studies of land surface processes. It has been developed by Lund University in a collaboration also involving the Potsdam Institute for Climate Impact Research and the Max-Planck Institute for Biogeochemistry, Jena, however, it is employed by a wide range of users worldwide. LPJ-GUESS belongs to the class of dynamic global vegetation models (DGVMs), which means that given spatially resolved data on climate and environmental conditions and on atmospheric carbon dioxide concentrations, it can predict structural, compositional and functional properties of the native and, depending on the input data, anthropogenic ecosystems of major climate zones of the Earth. Vegetation is dynamically simulated as a series of replicate patches, in which individuals of each simulated plant functional type (or species) compete for the available resources of light and water, as prescribed by the climate data.

The default output variables include for natural vegetation the composition and cover in terms of major species or plant functional types (PFTs), leaf area index (LAI), biomass and soil organic matter carbon pools, nitrogen pools, as well as component fluxes of CO₂, CH₄ and N₂O. Since here, the component fluxes are of interest, the calculation of these fluxes is briefly detailed in the following.

Primary production and plant growth follow the approach of LPJ-DGVM (Sitch et al. 2003) where canopy fluxes of carbon dioxide and water vapour are calculated by a coupled photosynthesis and stomatal conductance scheme based on the approach of BIOME3 (Haxeltine & Prentice 1996). The net primary production (NPP) accrued by an average individual plant each simulation year is allocated to leaves, fine roots and, for woody PFTs, sapwood, following a set of prescribed allometric relationships for each PFT, resulting in biomass, height and diameter growth (Sitch et al. 2003). Population dynamics (recruitment and mortality) are represented as stochastic processes, influenced by current resource status, demography and the life history characteristics of each PFT (Hickler et al. 2004). Biomass-destroying disturbances (such as wind fall or pests) are simulated as a stochastic process. In addition, wildfires are modelled prognostically based on temperature, fuel (litter) load and moisture. Litter arising from phenological turnover, mortality and disturbances enters the soil decomposition cycle.

LPJ-GUESS includes an interactive nitrogen cycle that significantly influences primary production of vegetation, decomposition of soil organic matter (SOM), and the release of greenhouse gases such as CO_2 and N_2O . An overview of the plant and soil N cycle as implemented within LPJ-GUESS is shown in Figure 4.

Nitrogen enters the ecosystem via nitrogen deposition (single bulk value encompassing wet and dry deposition) and biological nitrogen fixation (BNF) and fertilisation. Nitrogen deposition is prescribed as monthly mean values from an external database (Lamarque et al., 2011, 2013), whereas BNF is

computed prognostically based on an empirical dependency on ecosystem evapotranspiration derived from Cleveland et al. (1999).

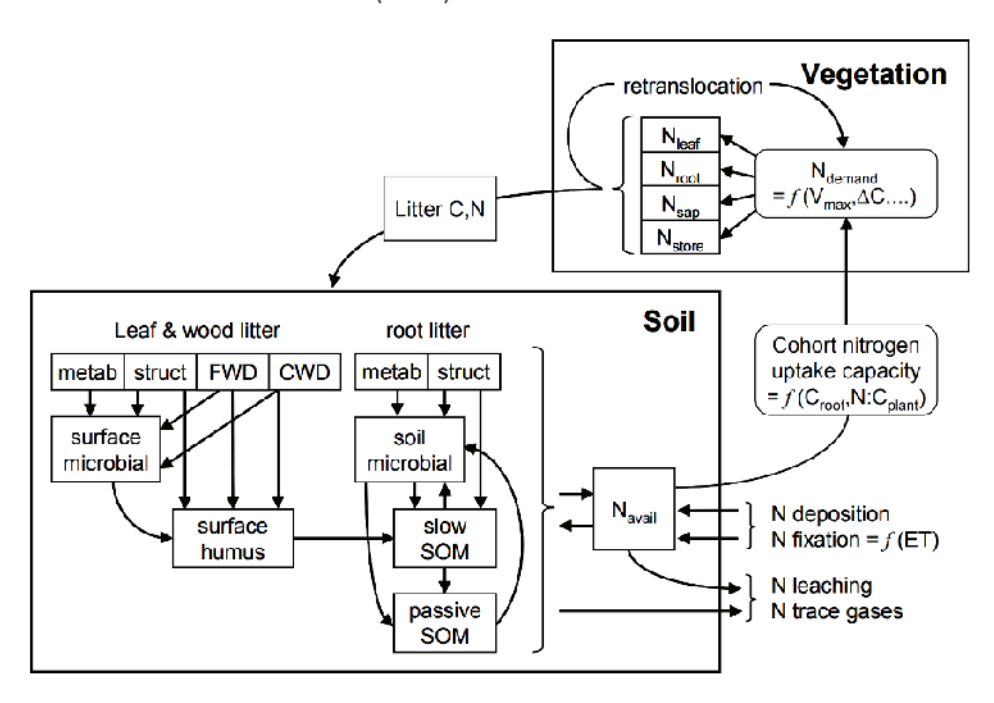


Figure 4: Schematic overview of N cycle in LPJ-GUESS. Abbreviations: FWD = fine woody debris; CWD = coarse woody debris; Navail = soil mineral N pool; Nleaf =leaf N mass; Nroot = fine root N mass; Nsap = sapwood N mass; Nstore =plant labile N store; Ndemand = daily plant N demand; Vmax = canopy rubisco capacity; ΔC = daily biomass increment; N:Cplant = aggregate N:C mass ratio for leaves and fine roots; ET = actual evapotranspiration. See Smith et al. (2014) for further details.

Along with nitrogen released through net mineralization during SOM decomposition, the available nitrogen (NH_4 and NO_3) for vegetation can be determined. Vegetation nitrogen demand is based on the carboxylation capacity of Rubisco, which maximizes net assimilation of leaves given the current temperature, light interception, and intercellular CO_2 concentration. From the optimal nitrogen concentration of leaves nitrogen demand of other vegetation compartments can be determined. If the available nitrogen cannot meet this demand, primary production is reduced. Vegetation litter contributes to the SOM pools, with a fraction of nitrogen being resorbed by vegetation before litter drop. The SOM scheme follows the CENTURY approach (Parton et al. 1993). If available nitrogen cannot meet microbial nitrogen demand during SOM decomposition, the decomposition rate is reduced. Available N is also affected by ammonification, nitrification, and denitrification processes (Xu-Ri and Prentice 2008), which emit NH_3 , NO, N_2O , and N_2 .

Additionally, nitrogen is lost from the ecosystem via leaching, computed daily as the sum of leached soluble organic nitrogen and leached mineral nitrogen, and through volatilisation by wildfires. In addition, 1 % of daily nitrogen mineralisation is assumed to be lost as gaseous emissions from soils (Thomas et al., 2013). Leaching of soluble organic nitrogen and carbon is computed conjointly as a fraction of the soil microbial soil organic matter nitrogen and carbon pools, dependent on soil water percolation and soil sand fraction, following Parton et al. (1993).

Carbon and nitrogen dynamics of soils are simulated conjointly by a soil organic matter scheme adopted from the CENTURY model (Parton et al. 2010). Decomposition of 11 SOM compartments differing in C:N stoichiometry and resistance to decay results in respiration (release of CO₂) and transfer of carbon and nitrogen between pools, satisfying mass balance.

4.1.1 CO₂ simulations

For the calculation of the CO₂ fluxes we use a model version (LPJ-GUESS version 4.0, revision 6562), that includes the functionality to simulate the diurnal cycle of the gross fluxes (GPP, autotrophic and heterotrophic respiration) based on the hourly temporal resolution of the input data. Traditionally, LPJ-GUESS only supports daily and annual processes, and for this the hourly input data are aggregated to daily values. The resulting fluxes are then interpolated to hourly values using hourly meteorological data. We use hourly air temperature, precipitation and incoming shortwave radiation derived from the ECMWF Reanalysis v5 (ERA5) product at a spatial resolution of 0.5 x 0.5 degrees. Annual Atmospheric CO₂ concentration are sourced from Keeling and Whorf (2005) prior to 1959 and from the Mauna Loa CO₂ record (NOAA Global Monitoring Laboratory, available at https://gml.noaa.gov/ccgg/trends/data.html) thereafter. Nitrogen deposition data are obtained from Lamarque et al (2011). Soil properties are derived from Harmonized World Soil Database v1.2 (https://www.fao.org/soils-portal/data-hub/soil-maps-and-databases/harmonized-world-soil-database-v12/en/). For this CO₂ fluxes simulation the LPJ-GUESS model is run for only natural (trees and grasses) land cover.

4.1.2 CH₄ simulations

European terrestrial CH_4 emissions and uptake are simulated using LPJ-GUESS (version 4.1, revision 12177). Here, the model is driven by daily air temperature, precipitation, and incoming shortwave radiation derived from the ECMWF Reanalysis v5 (ERA5) product at a spatial resolution of 0.5 x 0.5 degrees. The inputs for CO_2 concentration, nitrogen deposition, and soil properties are consistent with those used in the CO_2 simulation mentioned above. Peatland distribution data is derived from the Corine Land Cover (CLC) dataset (https://land.copernicus.eu/en/products/corine-land-cover/clc2018), and the inundated land area from WAD2M (Zhang et al. 2020). Excluding peatlands and inundated wetlands, the remaining land is considered as mineral soil. This product includes CH_4 emissions from peatlands, emissions from inundated wetlands, and both emission and uptake from mineral soils.

CH₄ emissions from carbon-rich peatlands are simulated based on Wania et al. (2010). The processes including methane production, gas diffusion (O₂ and CH₄), plant-mediated gas transport, methane oxidation, and methane ebullition. Emissions from inundated soil are treated simply by assuming that a set fraction of the carbon respired is released as methane instead of CO₂, following the procedure by Spahni et al. (2011). Mineral soil with relatively high soil moisture content enables methanogenic archaea to produce CH₄. Spahni et al. (2011) used water filled pore space (WFP) to represent soil moisture, and above a certain threshold of WFP a fraction of the CH₄ generated within soil diffuses into the atmosphere without being oxidized. Mineral soil with low soil moisture content implies oxic conditions which allow bacteria to consume CH₄ (i.e. mineral soil uptake). The mineral soil uptake is calculated following the procedures outlined by Spahni et al. (2011) and Curry (2007), where the CH₄ uptake depends on the atmospheric CH₄ concentration, the CH₄ effective soil diffusion and the CH₄ oxidation rate. As input, we used soil moisture, soil temperature, and soil respiration data produced by the LPJ-GUESS ecosystem model from the simulation of peatland methane fluxes.

4.1.3 N₂O simulations

For calculation of the N₂O fluxes we use version v4.1 of the LPJ-GUESS model (Nord et al., 2021) adapted to be able to output daily nitrogen fluxes per land cover class (natural, agricultural and pasture). Daily climate input data were taken from the CRU JRA v2.2 dataset for 1901-2020 at 0.5° resolution (Harris, 2021). To get the ecosystem stocks in balance a spin-up period of 500 years was

used before the start of the historical period. During spin-up the first 30 year (1901-1930) of detrended historical climate data were iterated. For nitrogen deposition input, monthly data were used (Lamarque et al. 2013) where the wet deposition was distributed based on precipitation amounts.

For separating the fluxes by land-use, CMIP6 data at 0.5° resolution were used (Hurtt et al., 2020). In these data land-use is divided into, urban, pasture, cropland, natural, peatland and barren. Of these land-use types pasture, cropland and natural were simulated based on yearly fractional cover data from 1850. The cropland is further divided into:

- "CC3ann" C3 annual, in LPJ-GUESS mapped as winter wheat (no inter-crop grass)
- "CC3per" C3 perennial, in LPJ-GUESS mapped to summer wheat with inter-crop grasses enabled
- "CC3nfx" C3 nitrogen fixer, in LPJ-GUESS mapped to summer wheat (no inter crop grass)
- "CC4ann" C4 annual, in LPJ-GUESS mapped to corn (no inter crop grass)
- "CC4per" C4 perennial, in LPJ-GUESS mapped to corn with inter crop grasses enabled where no inter crop grass means that outside of the plantation season bare soil is simulated.

In the land-use data there are also irrigated variants of these but they were not used. In addition, the dataset has yearly fertilization amounts from 1850 by crop type for the cropland, that were also used as input for the simulations. The natural class (which represents forest) was run without forest management and with a disturbance interval set to 100 years.

4.2 Results

4.2.1 CO₂

Figure 5 shows a timeseries of the simulated daily (for better visualisation) gross and net fluxes aggregated over the European domain for the years 2010 to 2022. The net flux (Net Ecosystem Exchange, NEE) is the difference between the two gross fluxes (Gross Primary Productivity, GPP, minus ecosystem respiration, RECO), positive values represent an uptake of CO_2 by the terrestrial vegetation from the atmosphere. The average annual sink term for our European domain has a value of 433 TgC yr⁻¹, which is comparable to a recent estimate from bottom up models in a synthesis study of the European carbon balance (389 Tg C yr⁻¹ average over the years 2010-2019; Lauerwald et al., 2024).

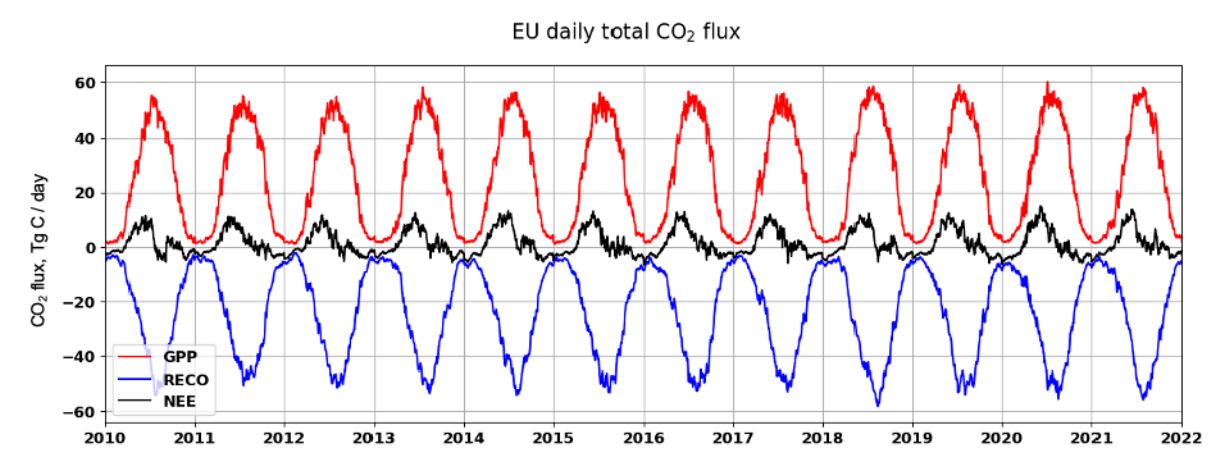


Figure 5: Timeseries of the simulated daily gross (GPP and RECO) and net (NEE) fluxes aggregated over the European domain for the years 2010 to 2022.

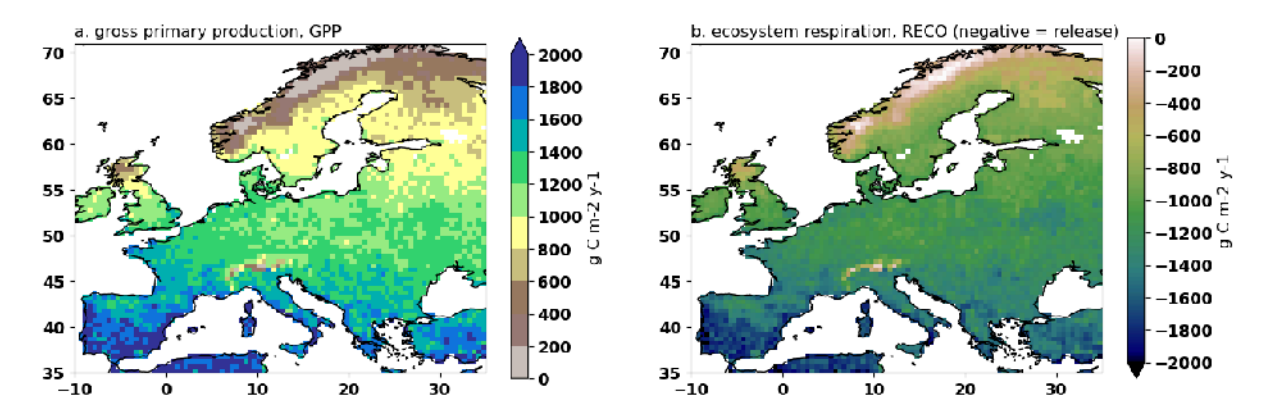


Figure 6: Spatial pattern of the annual gross fluxes (a showing GPP and b showing RECO) for 2010 for the European domain as simulated by LPJ-GUESS.

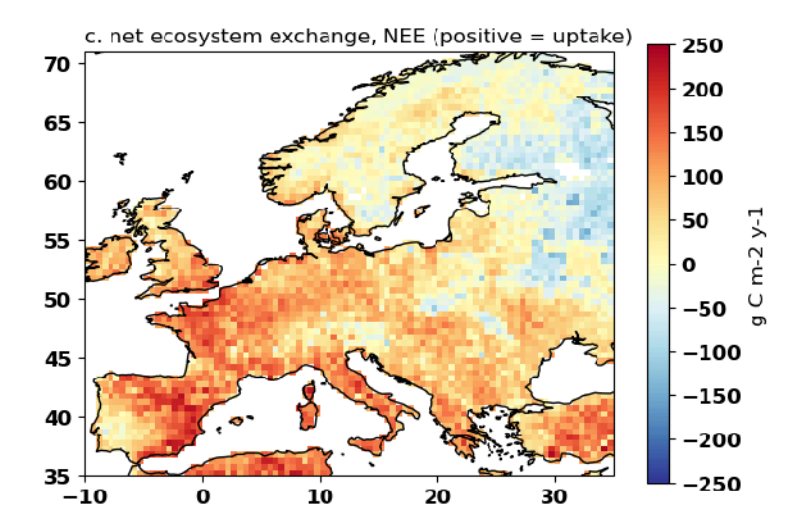


Figure 7: Spatial pattern of the annual net flux (NEE) for 2010 for the European domain as simulated by LPJ-GUESS.

Figure 6 and Figure 7 display the spatial patterns of the annual gross and net CO_2 fluxes at the 0.5° resolution for the year 2010. For the gross fluxes there is a typical north-south gradient with larger fluxes (higher productivity and higher ecosystem respiration) in southern Europe compared to northern Europe. In terms of NEE, the highest uptake of C is located in Western Europe, while Scandinavia and Eastern Europe is close to neutral and southern Finland and the European part of Russia is a small source (release to the atmosphere) of C. Most of the inverse modelling systems in WP2 will use the NEE as prior flux estimates.

4.2.2 CH₄

For CH₄, Figure 8 displays daily values of the four CH₄ flux components (emissions from peatlands, inundated wetlands and mineral soils, and uptake by mineral soils) from LPJ-GUESS aggregated over the European domain for the years 2010-2021. The figure also shows, for comparison, the same flux components as simulated by JSBACH-HIMMELI (Reick et al 2013; Raivonen et al., 2017; Susiluoto et al., 2018) because the uptake and release of CH₄ by mineral soils is a new feature in LPJ-GUESS that has not been extensively evaluated so far. The emission from peatland from LPJ-GUESS (red line) shows slight overestimates compared to JSBACH-HIMMELI (red dots), the overestimate mainly takes place in east EU which is partly due to the different peatland land cover used in these two models.

The emission from inundated wetland (blue line and dot) from the two models agree well. The emission from mineral soil from LPJ-GUESS (orange line) is underestimated compared to JSBACH-HIMMELI (orange dots). The underestimate mainly occurs in west and middle EU, which is expected due to the threshold setting for determining the emission. The uptake from mineral soil agree in magnitude, while the seasonality are different between the two models.

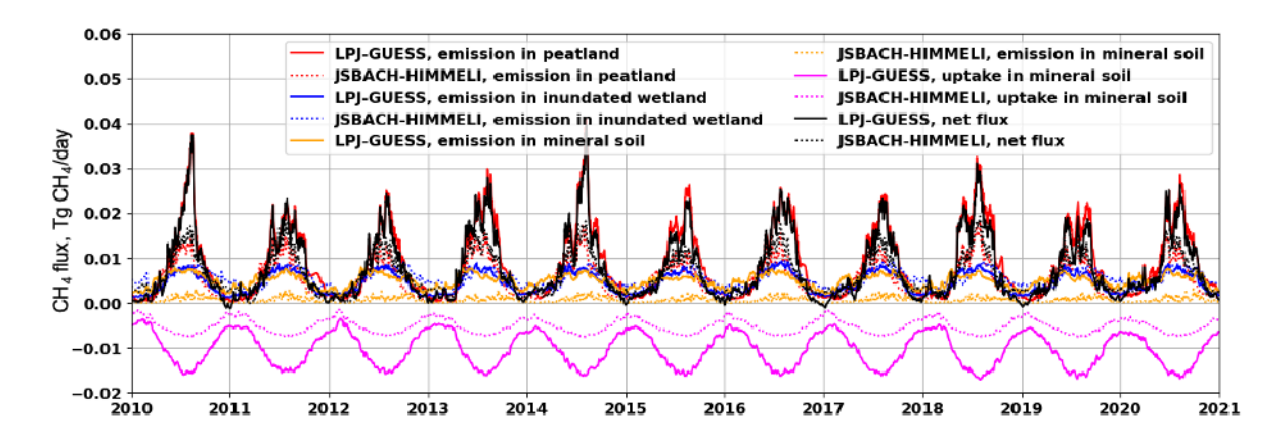


Figure 8: Daily CH₄ flux components from LPJ-GUESS aggregated over the European domain as well as the same simulated fluxes from JSBACH-HIMMELI for comparison.

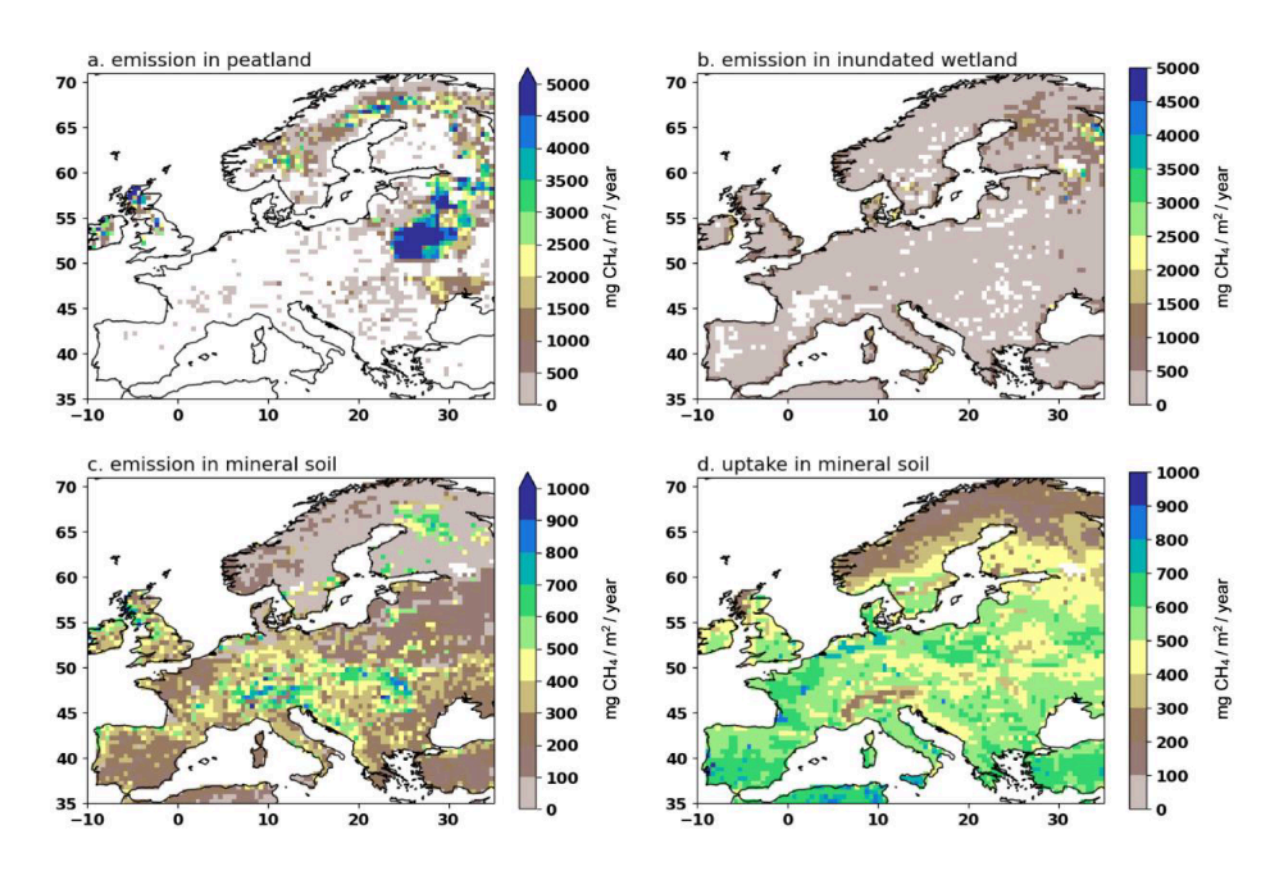


Figure 9: Spatial distribution of the four annual flux component values (a. peatland emissions, b. emissions from inundated wetlands, c. emissions from mineral soils, d. uptake by mineral soils) for 2010 from LPJ-GUESS.

Figure 9 displays the spatial patterns of the four flux components as annual CH_4 fluxes at the 0.5° resolution for the year 2010. Emissions from peatlands are clearly the largest flux component and mostly located in Eastern Europe and Scandinavia while the second largest emissions from inundated

wetlands are more homogeneously distributed over Europe. Emissions and uptake by mineral soils are minor components and mainly relate to the moisture status of the soil with a clear distinction between high latitudes (>60 N) and the rest of the domain (this is more pronounced to the uptake of CH₄ by mineral soils).

4.2.3 N₂O

For N_2O we mainly present results for the emissions from natural lands (forests, i.e. non pasture and non croplands) because emissions from land use for croplands and pastures are accounted for by the national inventory data. To avoid double counting, for croplands and pastures we will take the values provided by the inventory data as prior values in the inversion systems and not the emissions simulated by LPJ-GUESS. Figure 10 shows a timeseries of the annual N_2O emissions from forests for Germany over the years 2000 to 2020. There is clearly some interannual variability in these emissions which are caused by both changes in the atmospheric input of nitrogen (deposition) but also interannual variability in the meteorological forcing data. illustrates the variability of the natural land (forest) N_2O emissions per country for five selected years (2000, 2005, 2010, 2015 and 2020). Again there is clearly interannual variability in the N_2O emissions but even more pronounced are the differences in the emissions per country which can partly be explained by the size of the country (larger countries in size show in general larger emissions) but there are also some countries where the total emissions are determined by other factors, for instance the UK have very low emissions for their size.

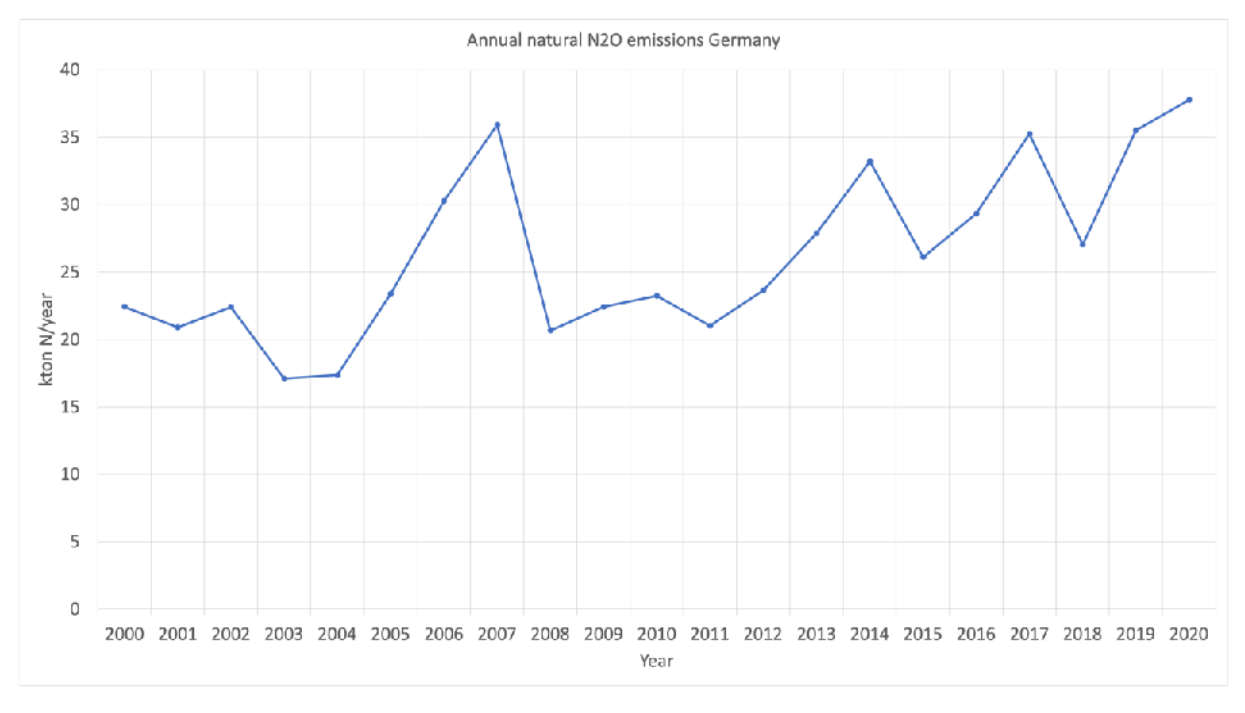


Figure 10: Timeseries of the annual N_2O emissions from land covered by natural vegetation (forests, i.e. non pastures and non croplands) in Germany.

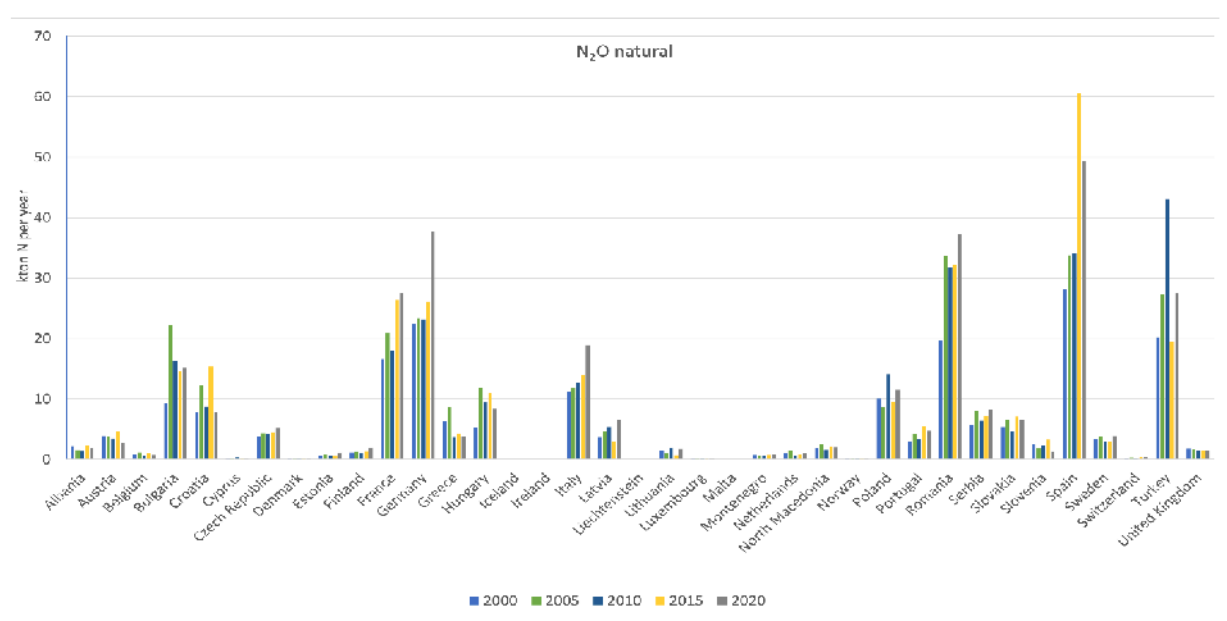


Figure 11: Snapshots of annual N_2O emissions from natural lands (forests) aggregated to the national levels for all countries covering the European domain for the years 2000, 2005, 2010, 2015 and 2020

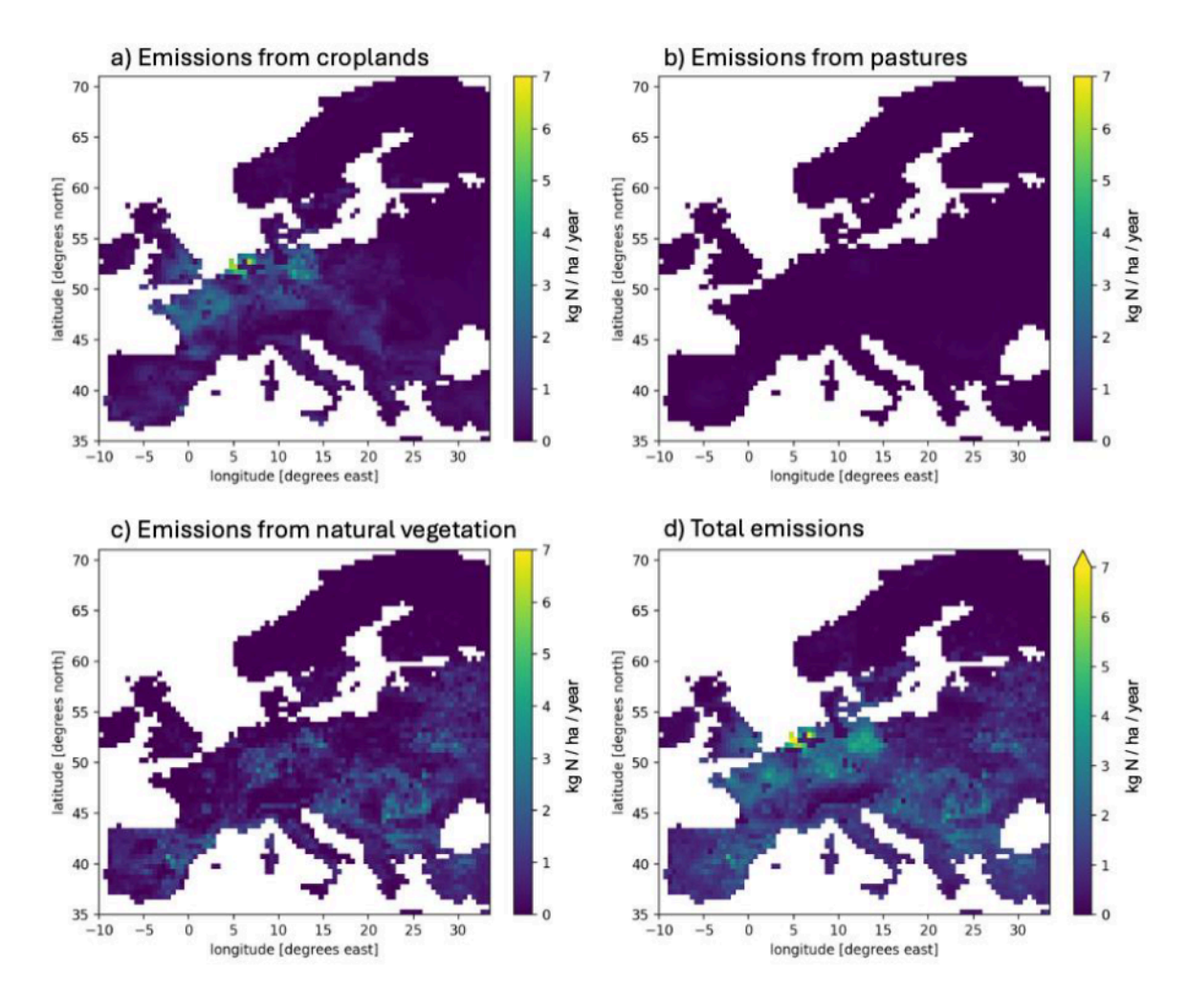


Figure 12: Spatial distribution of the annual average N_2O emission for the three different land cover types (a) croplands, b) pastures and c) natural vegetation) in a gridcell as well as the total emission per gridcell in kgN/ha simulated by LPJ-GUESS.

To illustrate the different magnitudes of the N_2O emissions from the different land cover types, Figure 12 displays the spatial patterns of the N_2O emissions per land cover type (plates a) to c)) as well as the total N_2O emissions as an annual average over the years 2010 to 2020. Clearly, emission from pastures show the smallest N_2O emissions whereas croplands show the highest N_2O emissions. N_2O emissions from croplands are mainly located in Western Europe (Germany, Benelux and France) corresponding to the areas of intensive agricultural activities. Natural emissions are dominated by forested areas in the temperate regions while N_2O emissions from boreal forest areas (Fennoscandinavia) are much smaller.

5 Temporal and vertical profiles of anthropogenic fluxes

The anthropogenic emission inventory, as described in section 3, provides annual total emissions per grid cell or point source. To convert these annual totals to higher temporal resolution input for the models (e.g. hourly emission), we provide temporal emission profiles by source sector, by country . Furthermore, sector-specific vertical profiles to describe emission height are needed for atmospheric modelling, which is mainly relevant for point source emissions.

5.1 Temporal profiles

Temporal profiles have been created per GNFR category used in AVENGERS and are available on the AVENGERS fileshare. For most categories, we provide monthly (day in month), weekly (day in week), and hourly (hour in day) profiles.

Table 2 in the Appendix shows an overview of the origin of all time profiles provided. The temporal profiles are often based on CAMS-REG-TEMPO v3.2 (Guevara et al., 2021). The original data contains country-specific monthly and weekly temporal profiles for air pollutants which are assumed to be representative for each year. For this deliverable, the profiles have been made by selecting the time profile of the pollutant that is most representative or an average of several pollutants. For some sectors, new temporal profiles have been created. These are described in more detail below.

For most sectors, the emission per hour of the year can be calculated by combining the time profile for month of the year, day of the week and hour of the day. For solid waste disposal and residential combustion, the emission per hour of the year can be calculated by combining the time profiles for day of the year and hour of the day. For these sectors the temporal breakdown is described by day of the year because the emission or activity is driven by meteorological parameters like temperature or atmospheric pressure.

5.1.1 CO₂

For CO₂, more specific temporal profiles were created for GNFR A, C and G.

For the energy sector (GNFR A) specific temporal profiles were developed in the CoCO2 project (https://atmosphere.copernicus.eu/node/865) and these contain country-specific weekly and monthly profiles for CO₂.

For GNFR C profiles were made for the years 2010-2021 using the degree day method (e.g., Mues et al., 2014). For this we use IFS forecasts of the 2-meter temperature, averaged for each country (using a global country mask) and day. The degree day calculation requires a temperature threshold above which no heating takes place and a constant fraction of non-heating related energy consumption. Although these numbers may differ between countries there is no consensus on the actual numbers per country. Here, we use a temperature threshold of 15 °C and a fraction for non-heating related energy consumption of 0.2. Hourly temporal profiles are based on the default TNO profiles.

Finally, for shipping (GNFR G), weekly profiles are based on the co-emitted species CO, but the monthly profiles are available specifically for CO₂ (following the same methodology as for the air pollutants).

5.1.2 CH₄

For CH₄, more specific temporal profiles were created for emissions from solid waste disposal (GNFR Js) and waste water treatment plants (Jww).

The temporal profile for solid waste disposal consists of day per year profile per 1°x1° grid cell. The temporal profile is based on the relation between the change in baroclinic pressure per hour and grid cell and the methane release as derived within the HoTC project (Banzhaf et al. in preparation) following a field study by Kissas et al. (2022). A daily average per grid cell was calculated from the resultant hourly temporal profiles.

For waste water treatment plants, a monthly temporal emission profile has been created. This is based on greenhouse gas emission estimates for winter and summer, from Asadi & McPhedran (2021). From this data we derived estimates for 4 month groups; November-February, March-April, May-August, and September-October. Separate profiles were created for both N_2O and CH_4 .

5.1.3 N₂O

New temporal profiles were created for N_2O from wastewater treatment plants (GNFR Jww), N_2O emissions from agriculture non-livestock (GNFR L AgriOther), indirect N_2O emissions from leaching and runoff (GNFR Lil and GNFR Kil), and indirect N_2O emissions from atmospheric deposition (GNFR Lid and GNFR Kid). The monthly temporal profiles for these sectors are presented in Figure 13 and the monthly N_2O emissions for all GNFR categories for the EU27+ are presented in Figure 14.

The monthly wastewater treatment plants profile for N_2O has been created using a similar method as the CH_4 profile as described before, using emission estimates from Asadi & McPhedran (2021).

For N_2O from agriculture (non-livestock), we used the profile for NH_3 for GNFR L from CAMS-REG-TEMPO v3.2 (Guevara et al., 2021) as base, as N_2O emissions are related to manure management activity. However, N_2O emissions are also affected by other environmental factors (temperature, precipitation, soil characteristics etc) and the sharp peak as seen in the NH_3 profiles is not very likely to occur for N_2O at exactly the same time. Therefore, we have flattened this monthly profile, by averaging for three periods in a year (March-May, June-October, November-February).

For indirect emissions from leaching and runoff, we based our temporal profile on modelled monthly emission estimates, by Wang et al. (2023). From this data, monthly temporal profiles per country were obtained.

A temporal profile for indirect emissions from atmospheric deposition was obtained using a monthly modelled NH_3 deposition map, resulting from a LOTOS-EUROS (LOTOS-EUROS v2.3.000 with emissions from CAMS REG 6.1 for the year 2019) run for 2019. This is the same deposition map as was used for created the proxy-map for indirect emissions from atmospheric deposition. Similar to the temporal profile for N_2O from GNFR L, we have flattened the profile, by averaging for three periods in a year (March-May, June-October, November-February).

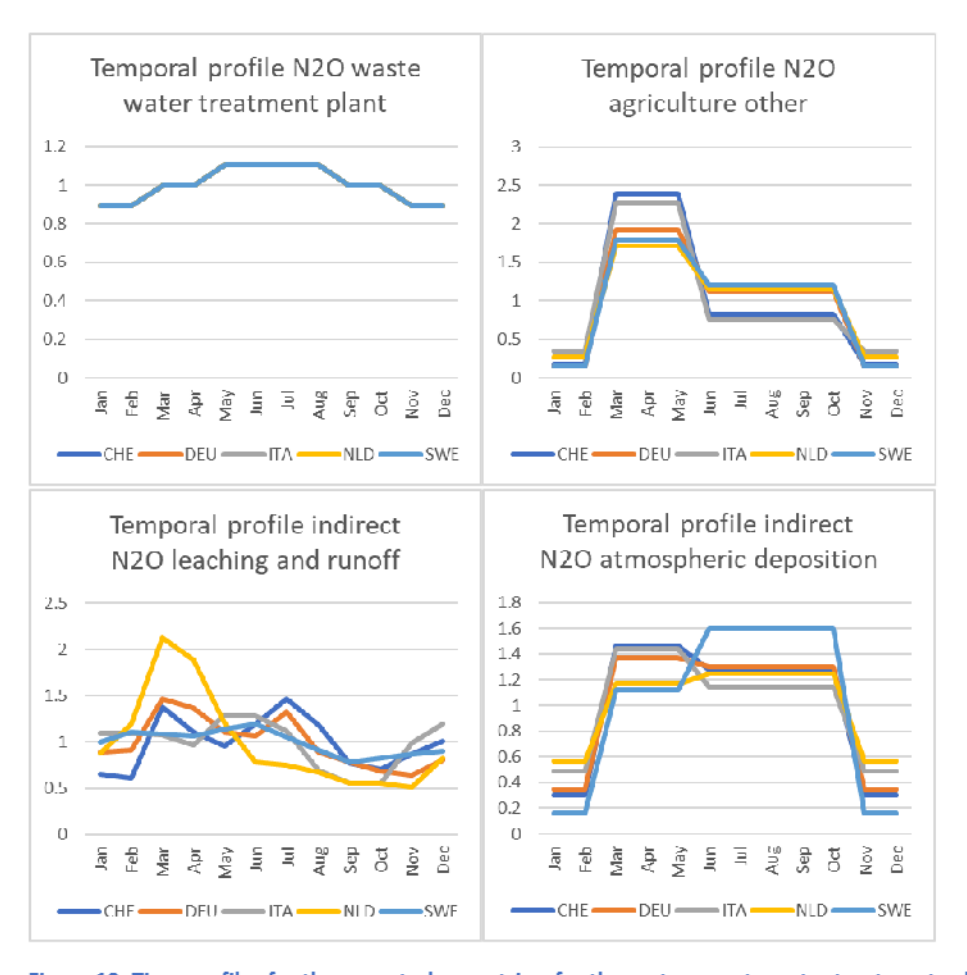


Figure 13: Time profiles for the case study countries, for the sectors waste water treatments plants, agriculture other, indirect N_2O from leaching and runoff and indirect N_2O from atmospheric deposition.

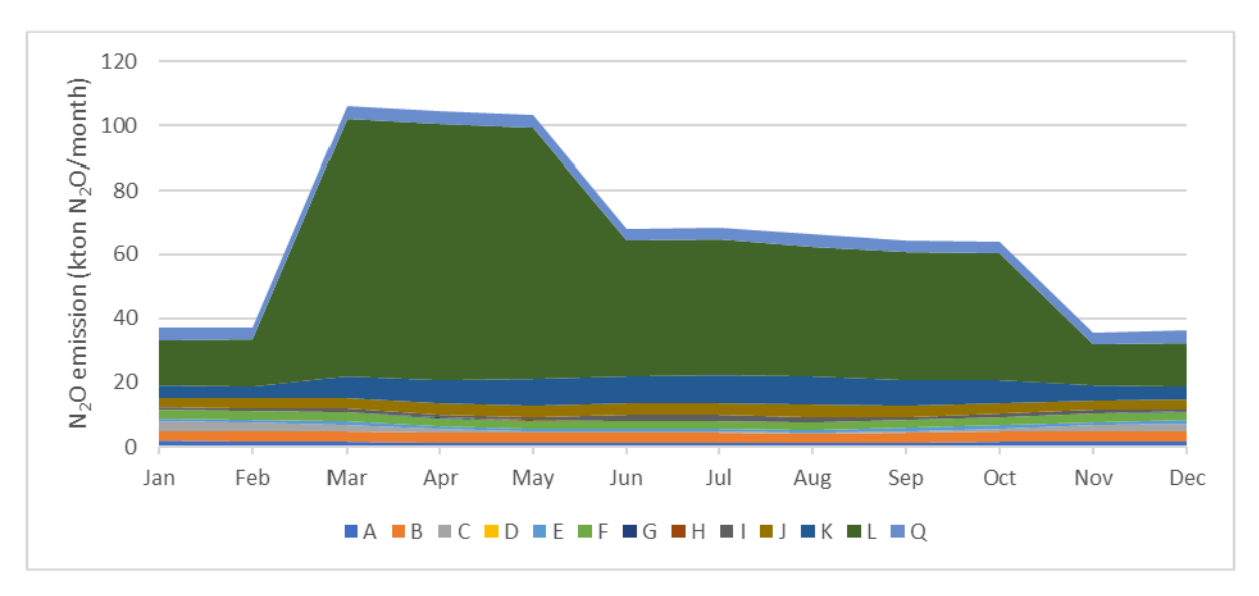


Figure 14: N₂O emission (kton) per month and per GNFR category for EU27+ (EU, and Norway, Iceland, Switzerland and United Kingdom)

5.2 Vertical profiles

As for the temporal profiles, vertical profiles have also been created for each GNFR sub-category as defined in AVENGERS. The vertical profiles include height from stacks and plume rise together. They are based on the vertical profiles as used in CAMS-REG_v7, but edited to align with sources of CO_2 , CH_4 and N_2O emissions. This also leads to slight variations in vertical profiles between the different compounds. For example, fugitive emissions (GNFR D) for CO_2 are mostly emitted from chimneys, whereas fugitive emissions for CH_4 are mostly emitted from mine shafts by active ventilation at a much lower elevation. For GNFR D, the default profile from CAMS-REG_v7 is used for CO_2 and N_2O , while a new profile has been assumed for CH_4 (20% in 0-20 meter and 80% in 20-92 meter).

6 Prior uncertainties of anthropogenic fluxes

In addition to prior anthropogenic fluxes, the top-down estimations require information on prior uncertainties.

6.1 Methodology

A detailed description of the methodology can be found in Super et al. (2024) and we only provide a short summary here. We have extended the work described in Super et al. (2024) with CH_4 and N_2O and the uncertainties apply to the European inventory (not the country-specific inventories).

Uncertainties in activity data and emissions factors for all relevant IPCC sectors were gathered from the NIR reports for 2018 (reporting year 2020) for all countries that report these uncertainties and fall within the domain. Gap filling is applied in case uncertainties are missing for specific sectors/fuels (see Super et al., 2024) and finally uncertainties in country-level emissions are propagated to the GNFR sector level.

Uncertainties in the proxy maps used for the spatial down-scaling are estimated assuming two sources of uncertainty. The first source is the data quality and this uncertainty is estimated using meta data or literature describing comparisons to other data sets. The second source of uncertainty is how representative the proxy data are for the spatial patterns in emissions. These uncertainties are based on expert judgment. For example, population is a reasonable proxy for residential emissions. However, it is also used as a default proxy when sector-specific proxies are lacking and in that case the representativeness error is much higher. Together, these two uncertainties represent the uncertainty in the spatial down-scaling, resulting in uncertainties per grid cell.

Finally, a spatial error correlation length is calculated for each proxy map and a weighted average per GNFR sector is provided. This relates to the representativeness error, i.e. if we overestimate the emissions from heating in the city centre this is likely to affect all grid cells within the city centre more or less equally. Hence, the errors in neighbouring grid cells are correlated following an exponential decay, with zero correlation when the correlation length is reached (following Kunik et al., 2019).

NOTE: We are currently working on a method to make the gridded uncertainties consistent with the country-level uncertainties. Therefore, an update will be made to the data in a few months. This should ease the use of the uncertainties in inverse modelling.

In addition to the actual calculation of the uncertainties in the European gridded data we have also examined whether these uncertainties can be extended to other years and how prone the results are to errors/typos in the reported uncertainties.

6.2 Results

An impression of the uncertainties (95% confidence interval ranges) in greenhouse gas emissions per country is provided in Figure 15.

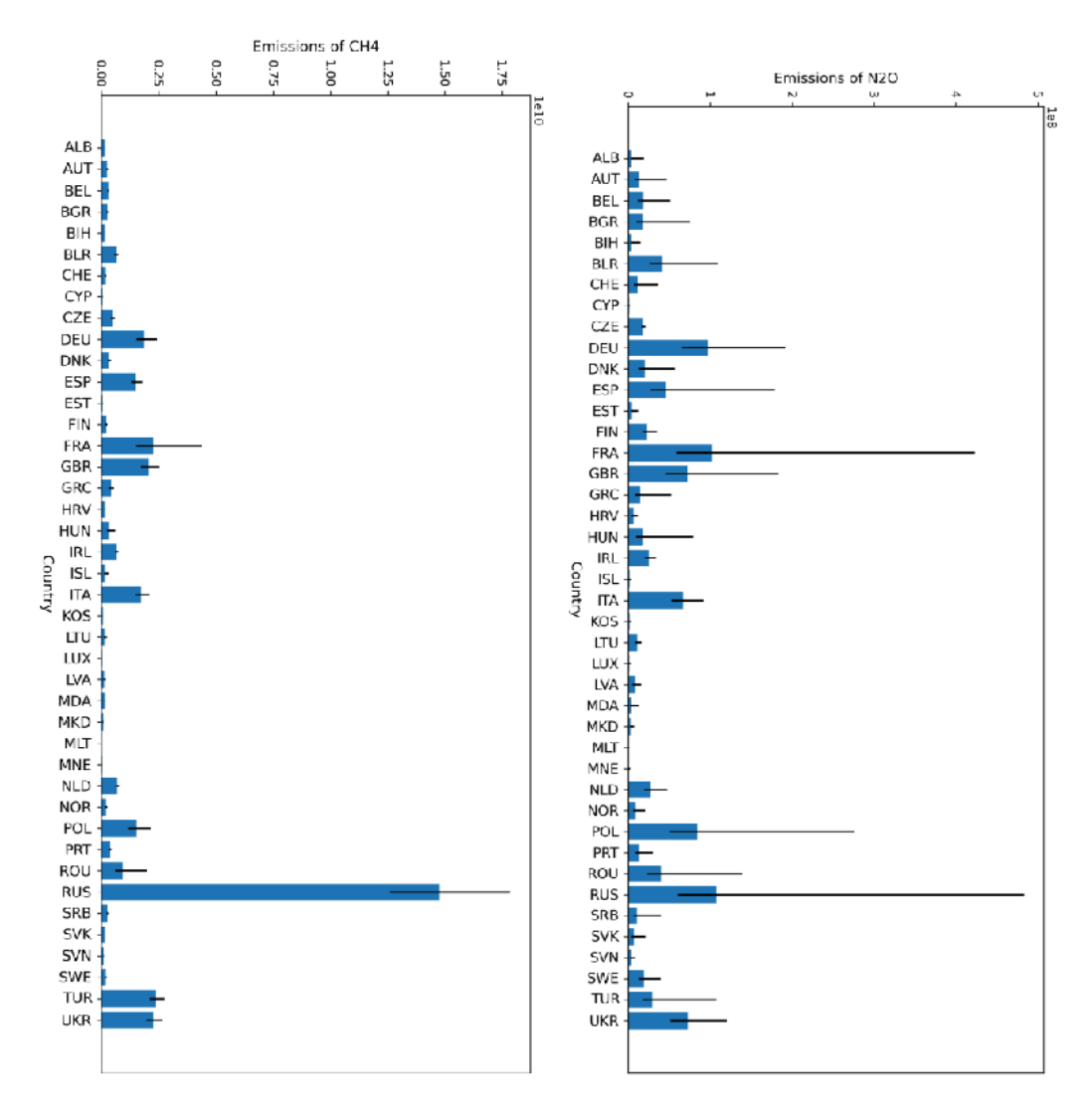


Figure 15. Emissions of CH₄ and N₂O and their 95% confidence interval per country.

A new addition is the inclusion of the LULUCF sector. For CH_4 and N_2O the net fluxes from LULUCF are not particularly large, although there is a significant uncertainty in these emissions and especially in the spatial distribution (Figure 16). For CO_2 the net LULUCF flux is an important contribution to the overall CO_2 flux and the net flux is negative (meaning a net uptake of CO_2). Since sub-sectors have their own spatial distribution we see cells with positive and negative fluxes, but also cells with very small net fluxes due to a combination of positive and negative fluxes at the same location. This results in grid cells with a very high relative uncertainty due to the division by a small number. Moreover, the aggregated fraction per grid cell can be large in order to get a large positive or negative flux from a small net flux. Although these numbers may seem physically strange they follow from the data and can be used as they are.

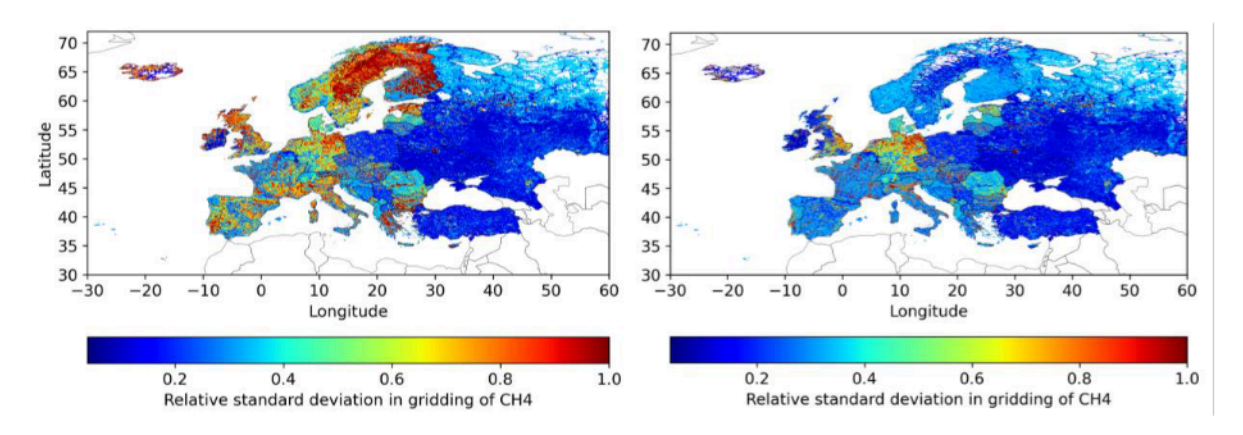


Figure 16. Maps of relative standard deviation in the spatial distribution of CH₄. At the left with LULUCF included and at the right without LULUCF.

To examine how representative these uncertainties are for other years we compared the reported uncertainties in 2020 to those reported in 2023 using the Dutch national emissions as a test case. Most of the uncertainties did change between 2020 and 2023 (73%); however, these changes were usually small (median 10.5 percentage points (p.p.)). Furthermore, larger changes in uncertainty generally occurred for IPCC categories with smaller emissions, while the uncertainties of IPCC categories with larger emissions barely changed (see Figure 17). Consequently, when emissions for IPCC categories were summed up to sector level, relevant changes in uncertainty (>3 p.p.) occurred mostly only for sectors with a small contribution (< 5%). Only one sector (AgriLivestock) had a contribution larger than 5% and a change in uncertainty larger than 3 p.p.

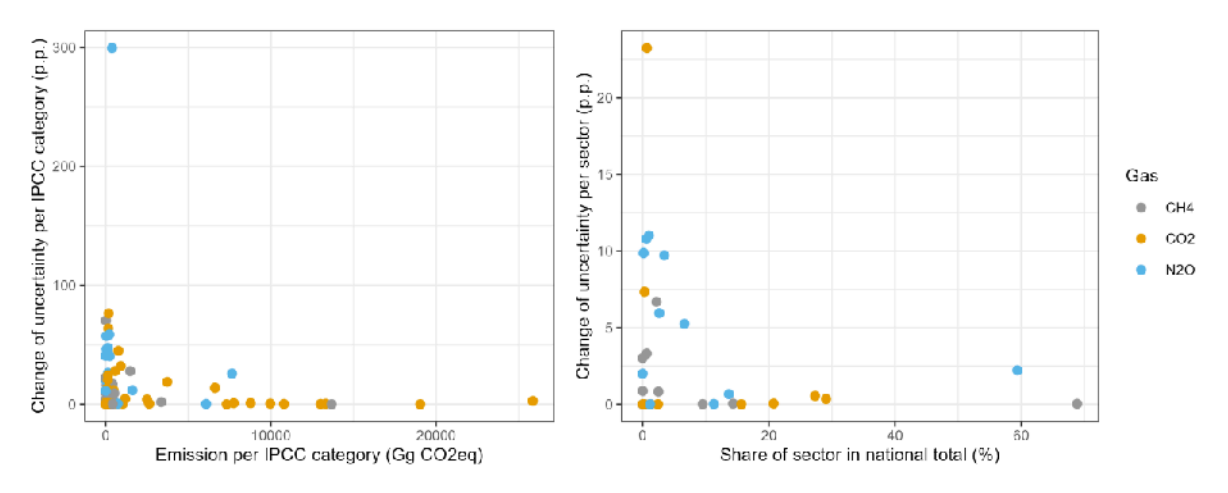


Figure 17. Change of uncertainty (in percentage points) per reported IPCC category against emissions per IPCC category (top) and change of uncertainty (in percentage points) per GNFR sector against share of this GNFR sector in total Dutch emissions for three greenhouse gases.

For Italy several typos were found in the NIR from 2020, which were corrected the year after. This results in a strong underestimation of the uncertainties in fugitive CH_4 emissions and an overestimation of the CO_2 emission uncertainties for GNFR C and GNFR B. In addition, the gap filling routine assigns a very high uncertainty to biomass combustion in some industrial sectors in Sweden. The reason for this is that an uncertainty for biomass is not provided and 'other fuels' are used, which have a high emission factor uncertainty.

The lesson we draw from this is that a comparison of several years and countries could be useful to find obvious mistakes or discrepancies in the reported uncertainties. In this project we are able to gather the data directly from the inventory agencies, which is an added value and resulted in these findings. Unfortunately, the data are normally provided as tables in PDF files, making it a tedious job, and prone to errors, to extract the data for all European countries over several years. It also requires expert knowledge to understand which values are actual outliers and when the data is based on country-specific conditions. This is not feasible outside of this project, requiring some short cuts (such as the gap filling routine), although it would help if data could be provided in a standardized format like the CRF tables. For now, we used the original reported uncertainties from 2020 to keep consistency between all countries.

References

Asadi, M., & McPhedran, K., 2021. Estimation of greenhouse gas and odour emissions from a cold region municipal biological nutrient removal wastewater treatment plant. *Journal of Environmental Management*, 281, 111864.

Banzhaf et al. (in preparation): "Improving the spatio-temporal variability of greenhouse gas emissions for North-Western Europe".

Cleveland, C. C., Townsend, A. R., Schimel, D. S., Fisher, H., Howarth, R. W., Hedin, L. O., Perakis, S. S., Latty, E. F., Von Fischer, J. C., Elseroad, A., and Wasson, M. F., 1999: Global patterns of terrestrial biological nitrogen (N2) fixation in natural ecosystems, Global Biogeochem. Cy., 13, 623–645, 1999.

Curry, C.L., 2007. Modeling the soil consumption of atmospheric methane at the global scale. Global Biogeochemical Cycles, 21(4).

Dammers, E., Tokaya, J., Mielke, C., Hausmann, K., Griffin, D., McLinden, C., Eskes, H., and Timmermans, R., 2022: Can TROPOMI-NO₂ satellite data be used to track the drop and resurgence of NO₂ emissions between 2019–2021 using the multi-source plume method (MSPM)?, Geosci. Model Dev. Discuss. [preprint], https://doi.org/10.5194/gmd-2022-292, in review, 2022.

Denier van der Gon, H., et al., 2023. Prior emission data 2021. Documentation. D2.2 from CoCO2 (Prototype system for a Copernicus CO2 service.

EDGAR, Global Greenhouse Gas Emissions database v8, https://edgar.jrc.ec.europa.eu/dataset_ghg80 , accessed may 2024

Englund, D., Arvelius, J., Windmark, F., Leung, W., Sundbom, M., Pettersson, E., Gerner, A., Guban, P., Hammerlid, D., 2024. Metod- och kvalitetsbeskrivning för geografiskt fördelade emissioner till luft. SMED Rapport nr 2 2024.

Guevara, M., Jorba, O., Tena, C., Denier van der Gon, H., Kuenen, J., Elguindi, N., Darras, S., Granier, C., and Pérez García-Pando, C., 2021: Copernicus Atmosphere Monitoring Service TEMPOral profiles (CAMS-TEMPO): global and European emission temporal profile maps for atmospheric chemistry modelling, Earth Syst. Sci. Data, 13, 367–404, https://doi.org/10.5194/essd-13-367-2021, 2021.

Harris, I.C., 2021: CRU JRA v2.2: A forcings dataset of gridded land surface blend of Climatic Research Unit (CRU) and Japanese reanalysis (JRA) data; Jan.1901 - Dec.2020. NERC EDS Centre for Environmental Data Analysis. University of East Anglia Climatic Research Unit. https://catalogue.ceda.ac.uk/uuid/4bdf41fc10af4caaa489b14745c665a6

Haxeltine, A. & Prentice, I.C., 1996. BIOME3: An equilibrium terrestrial biosphere model based on ecophysiological constraints, resource availability, and competition among plant functional types. Global Biogeochemical Cycles 10: 693-709.

Hickler, T., Smith, B., Sykes, M.T., Davis, M.B., Sugita, S. & Walker, K., 2004. Using a generalized vegetation model to simulate vegetation dynamics in the western Great Lakes region, USA, under alternative disturbance regimes. Ecology 85: 519-530.

Hurtt, G. C., Chini, L., Sahajpal, R., Frolking, S., Bodirsky, B. L., Calvin, K., Doelman, J. C., Fisk, J., Fujimori, S., Klein Goldewijk, K., Hasegawa, T., Havlik, P., Heinimann, A., Humpenöder, F., Jungclaus, J., Kaplan, J. O., Kennedy, J., Krisztin, T., Lawrence, D., Lawrence, P., Ma, L., Mertz, O., Pongratz, J.,

Popp, A., Poulter, B., Riahi, K., Shevliakova, E., Stehfest, E., Thornton, P., Tubiello, F. N., van Vuuren, D. P., and Zhang, X., 2020: Harmonization of global land use change and management for the period 850–2100 (LUH2) for CMIP6, Geosci. Model Dev., 13, 5425-5464, https://doi.org/10.5194/gmd-13-5425-2020, 2020.

Keeling C. and Whorf T., 2005 Atmospheric carbon dioxide record from Mauna Loa Trends: A Compendium of Data on Global Change. Carbon Dioxide Information Analysis Center (Oak Ridge, TN: Oak Ridge National Laboratory)

Kissas, K., Ibrom, A., Kjeldsen, P., Scheutz, C., 2022. Methane emission dynamics from a Danish landfill: The effect of changes in barometric pressure. Waste Manag. 138, 234–242. https://doi.org/10.1016/j.wasman.2021.11.043.

Kuenen, J., Dellaert, S., Visschedijk, A., Jalkanen, J.-P., Super, I., and Denier van der Gon, H., 2022. CAMS-REG-v4: a state-of-the-art high-resolution European emission inventory for air quality modelling, Earth Syst. Sci. Data, 14, 491–515.

Kunik, L., Mallia, D. V., Gurney, K. R., Mendoza, D. L., Oda, T., and Lin, J. C.: Bayesian inverse estimation of urban CO2 695 emissions: Results from a synthetic data simulation over Salt Lake City, UT, Elem. Sci. Anth., 7, 36. https://doi.org/https://doi.org/10.1525/elementa.375, 2019

Lamarque, J.-F., Dentener, F., McConnell, J., Ro, C.-U., Shaw, M., Vet, R., Bergmann, D., Cameron-Smith, P., Dalsoren, S., Doherty, R., Faluvegi, G., Ghan, S. J., Josse, B., Lee, Y. H., MacKenzie, I. A., Plummer, D., Shindell, D. T., Skeie, R. B., Stevenson, D. S., Strode, S., Zeng, G., Curran, M., Dahl-Jensen, D., Das, S., Fritzsche, D., and Nolan, M., 2013: Multi-model mean nitrogen and sulfur deposition from the Atmospheric Chemistry and Climate Model Intercomparison Project (ACCMIP): evaluation of historical and projected future changes, Atmos. Chem. Phys., 13, 7997–8018, doi:10.5194/acp-13-7997-2013, 2013.

Lamarque, J.-F., Kyle, G. P., Meinshausen, M., Riahi, K., Smith, S. J., van Vuuren, D. P., Conley, A. J., and Vitt, F., 2011: Global and regional evolution of short-lived radiatively-active gases and aerosols in the Representative Concentration Pathways, Climatic Change, 109, 191–212, 2011.

Lauerwald R. et al., 2024, Carbon and greenhouse gas budgets of Europe: trends, interannual and spatial variability, and their drivers. In revision, GBC, 2024

Mues, A., Kuenen, J., Hendriks, C., Manders, A., Segers, A., Scholz, Y., Hueglin, C., Builtjes, P., and Schaap, M., 2014: Sensitivity of air pollution simulations with LOTOS-EUROS to the temporal distribution of anthropogenic emissions, Atmos. Chem. Phys., 14, 939–955, https://doi.org/10.5194/acp-14-939-2014, 2014.

Nord, J., Anthoni, P., Gregor, K., Gustafson, A., Hantson, S., Lindeskog, M., Meyer, B., Miller, P., Nieradzik, L., Olin, S., Papastefanou, P., Smith, B., Tang, J., and Wårlind, D., 2021: LPJ-GUESS Release v4.1.1 model code, Zenodo, https://doi.org/10.5281/zenodo.8065737, 2021.

Parton, W. J., Hanson, P. J., Swanston, C., Torn, M., Trumbore, S. E., Riley, W., and Kelly, R., 2010: ForCent model development and testing using the Enriched Background Isotope Study experiment, J. Geophys. Res., 115, G04001, doi:10.1029/2009JG001193, 2010.

Parton, W. J., Scurlock, J. M. O., Ojima, D. S., Gilmanov, T. G., Scholes, R. J., Schimel, D. S., Kirchner, T., Menaut, J.-C., Seastedt, T., Garcia Moya, E., Kamnalrut, A., and Kinyamario, J. I., 1993: Observations and modeling of biomass and soil organic matter dynamics for the grassland biome worldwide, Global Biogeochem. Cy., 7, 785–809, 1993.

Raivonen, M., Smolander, S., Backman, L., Susiluoto, J., Aalto, T., Markkanen, T., Mäkelä, J., Rinne, J., Peltola, O., Aurela, M., Tomasic, M., Li, X., Larmola, T., Juutinen, S., Tuittila, E-S., Heimann, M., Sevanto, S., Kleinen, T., Brovkin, V., and Vesala T., 2017: HIMMELI v1.0: Helsinkl Model of MEthane buiLd-up and emlssion for peatlands, Geosci. Model Devel., 10, 4665-4691, https://doi.org/10.5194/gmd-10-4665-2017, 2017.

Reick, C., Raddatz, T., Brovkin, V. & Gayler, V., 2013: Representation of natural and anthropogenic land cover change in MPI-ESM. Journal of Advances in Modeling Earth Systems, 5, 459-482, https://doi.org/10.1002/jame.20022, 2013.

Schneider, C., Pelzer, M., Toenges-Schuller, N., Nacken, M., and Niederau, A., 2016: ArcGIS basierte Lösung zur detaillierten, deutschlandweiten Verteilung (Gridding) nationaler Emissionsjahreswerte auf Basis des Inventars zur Emissionsberichterstattung: Forschungskennzahl 3712 63 240 2, Texte, 71, 5, 2016

Sitch, S., Smith, B., Prentice, I.C., Arneth, A., Bondeau, A., Cramer, W., Kaplan, J., Levis, S., Lucht, W., Sykes, M., Thonicke, K. & Venevsky, S., 2003. Evaluation of ecosystem dynamics, plant geography and terrestrial carbon cycling in the LPJ Dynamic Global Vegetation Model. Global Change Biology 9: 161-185.

Smith, B., Prentice, I.C. & Sykes, M.T., 2001. Representation of vegetation dynamics in the modelling of terrestrial ecosystems: comparing two contrasting approaches within European climate space. Global Ecology & Biogeography 10: 621-637.

Smith, B., Wårlind, D., Arneth, A., Hickler, T., Leadley, P., Siltberg, J., and Zaehle, S., 2014: Implications of incorporating N cycling and N limitations on primary production in an individual-based dynamic vegetation model, Biogeosciences, 11, 2027-2054, https://doi.org/10.5194/bg-11-2027-2014, 2014.

Spahni, R., Wania, R., Neef, L., Van Weele, M., Pison, I., Bousquet, P., Frankenberg, C., Foster, P.N., Joos, F., Prentice, I.C. and Van Velthoven, P., 2011. Constraining global methane emissions and uptake by ecosystems. Biogeosciences, 8(6), pp.1643-1665.

Super, I., Scarpelli, T., Droste, A., and Palmer, P. I., 2024: Improved definition of prior uncertainties in CO2 and CO fossil fuel fluxes and the impact on a multi-species inversion with GEOS-Chem (v12.5), EGUsphere [preprint], https://doi.org/10.5194/egusphere-2023-2025, 2024.

Susiluoto, J., Raivonen, M., Backman, L., Laine, M., Mäkelä, J., Peltola, O., Vesala, T., and Aalto, T., 2018: Calibrating a wetland methane emission model with hierarchical modeling and adaptive MCMC, Geosci. Model Dev., 11, 1199–1228, https://doi.org/10.5194/gmd-11-1199-2018, 2018

Thomas, R. Q., Bonan, G. B., and Goodale, C. L., 2013: Insights into mechanisms governing forest carbon response to nitrogen deposition: a model—data comparison using observed responses to nitrogen addition, Biogeosciences, 10, 3869–3887, doi:10.5194/bg-10-3869-2013, 2013.

Wania, R., Ross, I. and Prentice, I.C., 2010. Implementation and evaluation of a new methane model within a dynamic global vegetation model: LPJ-WHyMe v1. 3. Geoscientific Model Development Discussions, 3(1), pp.1-59.

Wang, J., Vilmin, L., Mogollón, J.M., Beusen, A.H.W., van Hoek, W.J., Liu, X., Pika, P.A., Middelburg, J.J., and Bouwman, A.F., 2023. Inland waters increasingly produce and emit nitrous oxide. Environmental Science & Technology 2023 57 (36), 13506-13519.

Xu-Ri, and I. C. Prentice, 2008. Terrestrial Nitrogen Cycle Simulation with a Dynamic Global Vegetation Model. Global Change Biology 14 (8): 1745–64. doi:10.1111/j.1365-2486.2008.01625.x

Zhang, Z., Fluet-Chouinard, E., Jensen, K., McDonald, K., Hugelius, G., Gumbricht, T., Carroll, M., Prigent, C., Bartsch, A. and Poulter, B., 2020. Development of a global dataset of Wetland Area and Dynamics for Methane Modeling (WAD2M). Earth System Science Data Discussions, 2020, pp.1-50.

Annex 1 Temporal profiles

Table 2: Assumptions to derive temporal profiles for CO_2 , CH_4 and N_2O . For most sectors, the temporal profile of another pollutant from the CAMS-REG-TEMPO v3.2 is used. Temporal profiles marked with an * are described in more detail in section 5.1.

GNFR	GNFR Sector	CO ₂	CH ₄	N ₂ O
А	A & Af & Ab	Temporal profiles CO ₂ GNFR A*	NO _x GNFR A (CAMS-REG- TEMPO v3.2)	NO _x GNFR A (CAMS-REG- TEMPO v3.2)
В	B & Bf & Bb	CO GNFR B (CAMS- REG-TEMPO v3.2)	NO _x GNFR B (CAMS-REG- TEMPO v3.2)	NO _x GNFR B (CAMS-REG- TEMPO v3.2)
С	CD & Cf & Cb	Made using degree day method*	NO _x GNFR C (CAMS-REG- TEMPO v3.2)	NO _x GNFR C (CAMS-REG- TEMPO v3.2)
D	D	CO GNFR D (CAMS- REG-TEMPO v3.2)	Flat	NO _x GNFR D (CAMS-REG- TEMPO v3.2)
E	E	CO GNFR E (CAMS- REG-TEMPO v3.2)	Monthly: flat Weekly & hourly: NO _x GNFR E (CAMS-REG- TEMPO v3.2)	Monthly: flat Weekly & hourly: NO _x GNFR E (CAMS-REG- TEMPO v3.2)
F	F & Ff	NO _x GNFR F1 (CAMS- REG-TEMPO v3.2)	NMVOC GNFR F1 (CAMS- REG-TEMPO v3.2)	NO _x GNFR F2 (CAMS-REG- TEMPO v3.2)
G	G & Gf & Gb	Monthly: specific sea shipping profiles Weekly and hourly: CO GNFR G (CAMS- REG-TEMPO v3.2)	Inland shipping: flat profile Sea shipping: monthly has sea shipping profile. Weekly and hourly are flat.	Inland shipping: flat profile Sea shipping: monthly has sea shipping profile. Weekly and hourly are flat.
Н	H & Hb & Hf	CO GNFR H (CAMS- REG-TEMPO v3.2)	NO _x GNFR F (CAMS-REG- TEMPO v3.2)	NO _x GNFR F (CAMS-REG- TEMPO v3.2)
I	1 & lb & If	Average of CO and NO _x GNFR I (CAMS-REG-TEMPO v3.2)	Flat	NO _x GNFR I (CAMS-REG- TEMPO v3.2)
J	J & Jb & Jf	CO GNFR J (CAMS- REG-TEMPO v3.2)	Flat as in GNFR J (CAMS- REG-TEMPO v3.2)	Flat as in GNFR J (CAMS- REG-TEMPO v3.2)
	Jww	NA	Monthly: Waste water treatment plants profile (CH ₄) * Weekly and hourly: flat	Monthly: Waste water treatment plants profile (N ₂ O) * Weekly and hourly: flat
	Js	NA	Day in year for CH ₄ from solid waste disposal* Hourly: flat	NA
K	K & Kf	NA	Flat	NH₃ GNFR K (CAMS-REG- TEMPO v3.2)
	Kid	NA	NA	Monthly: Indirect N₂O from atmospheric deposition profile*

	Kil	NA	NA	Weekly & hourly: NH₃ GNFR K (CAMS-REG- TEMPO v3.2) Monthly: Indirect N₂O from leaching and runoff profile* Weekly & hourly: NH₃
				GNFR K (CAMS-REG- TEMPO v3.2)
L	L & Lf & Ld	CO GNFR L (CAMS- REG-TEMPO v3.2)	Flat	Monthly: N ₂ O from agriculture profile* Weekly & hourly: NH ₃ GNFR L (CAMS-REG- TEMPO v3.2)
	Lid	NA	NA	Monthly: Indirect N ₂ O from atmospheric deposition profile* Weekly & hourly: NH ₃ GNFR L (CAMS-REG- TEMPO v3.2)
	Lil	NA	NA	Indirect N ₂ O from leaching and runoff profile* Weekly & hourly: NH ₃ GNFR L (CAMS-REG- TEMPO v3.2)
Q	Qb, Qc, Qd, Qi, Qni, Qnm	Flat	Flat	Flat

Annex 2 First comparison for anthropogenic N₂O to EDGARv8.

Especially for N₂O the standard emission database used in modelling of anthropogenic N₂O emissions is EDGAR¹ because TNO did previously not provide gridded European N₂O emissions in Horizon projects or under the Copernicus Atmospheric Monitoring service (CAMS). Here we provide a first comparison between the TNO-GHGco_v7 N2O emission and the most recent version of EDGAR (https://edgar.jrc.ec.europa.eu/dataset_ghg80)

A first comparison for the five case study countries in AVENGERS (Switzerland, Germany, Italy, Netherlands and Sweden) is presented in Figure 18. As can be seen emission estimates for the 2005 – 2010 period are unstable in several countries but AVENGERS will only use the 2010-2021 timeseries in its inversions. After 2010 trends in both datasets are the same (and mostly flat). In Figure 19 a similar comparison is made for selected other European countries. In general trends are similar for all EU countries but non-EU can be very different (see Turkey as an example). For EU countries EDGAR is generally somewhat higher, for Spain almost factor 2 but exceptions exist as well, for example Switzerland and Italy are somewhat higher in the TNO dataset. There is a remarkable feature in EDGAR for some countries in 2012, see the uptick in emissions for the Netherlands and Turkey. At present we do not know the underlying reason for this.

For non-EU countries TNO is sometimes very different from EDGAR because the EDGAR emission estimates were taken from the GAINS model. In the near future we will evaluate the data for the NON_EU countries to decide on the best source of data for this region.

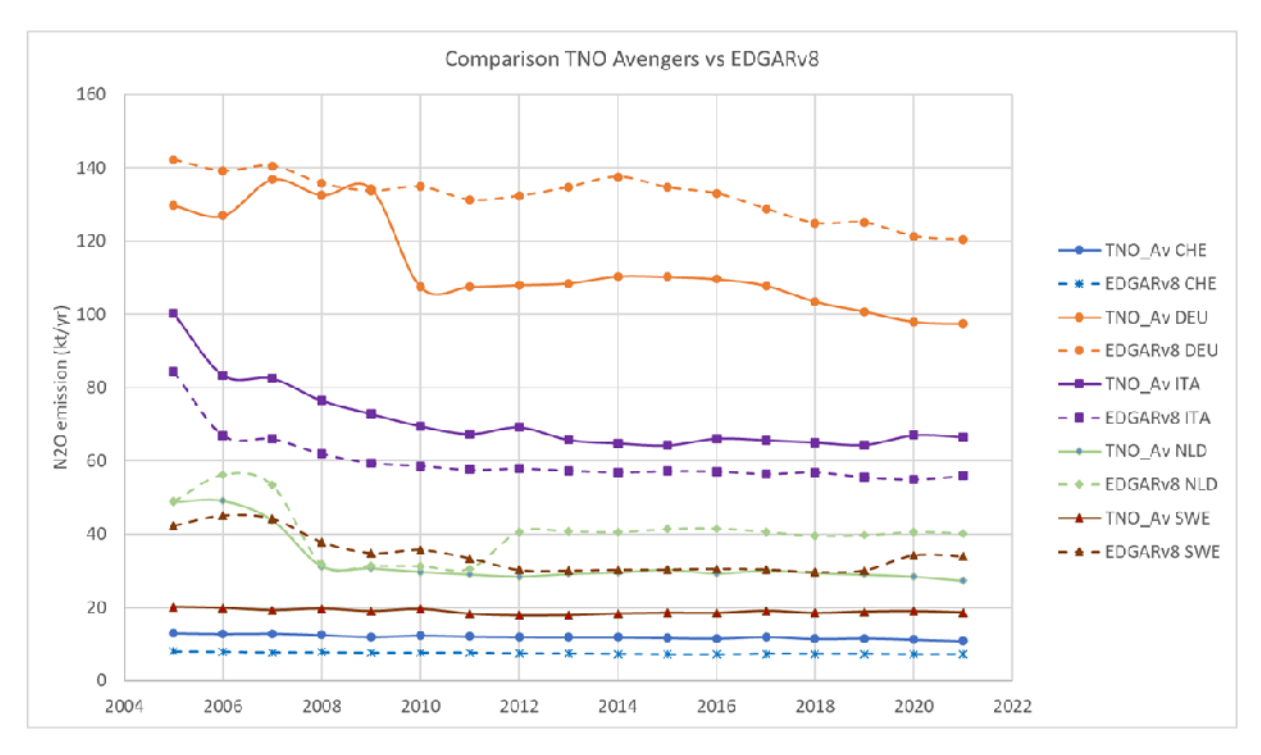


Figure 18 N₂O emission from TNO-GHGco_v7 and EDGARv8 from the five AVENGERS case study countries for the period 2005-2021.

.

¹ https://edgar.jrc.ec.europa.eu/

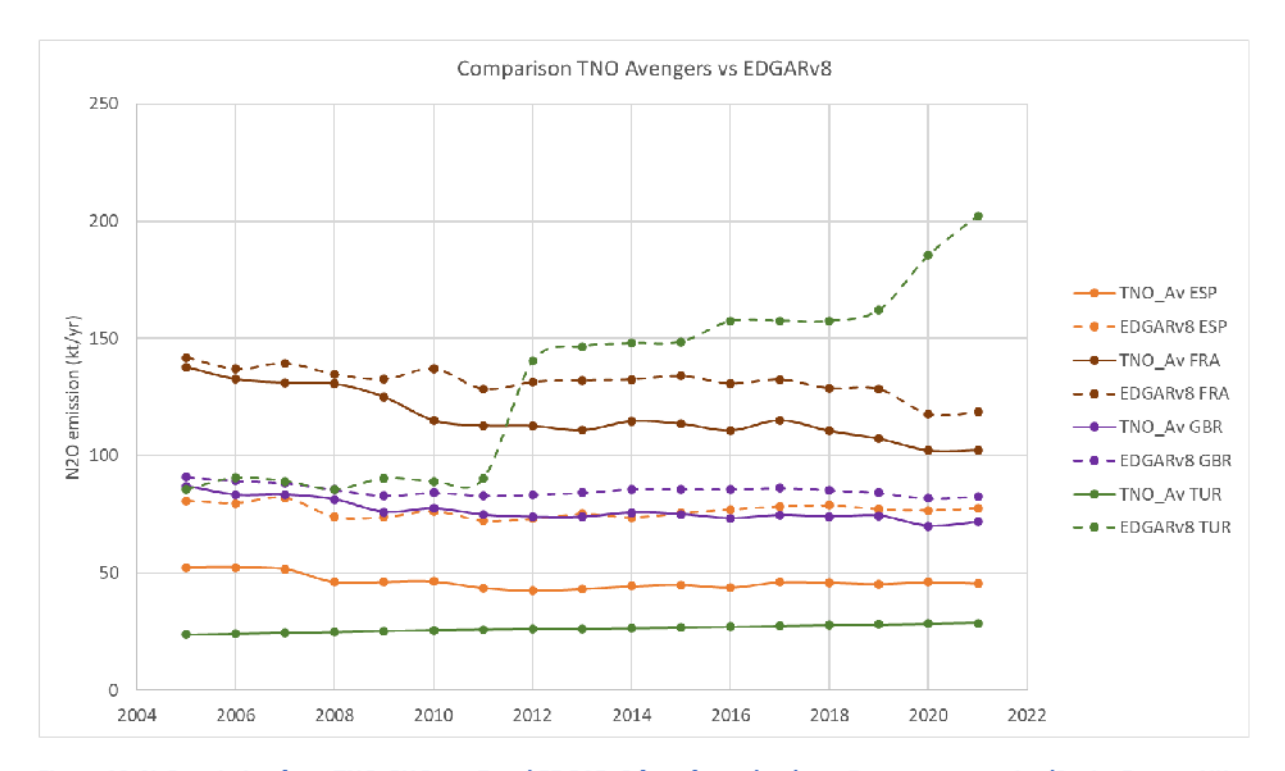


Figure 19 $\,\mathrm{N_2O}$ emission from TNO-GHGco_v7 and EDGARv8 for a few other large European countries (Spain, France, UK, Turkey) for the period 2005-2021.

The EDGARv8 data are available in monthly emission files. The emission temporal pattern is, however, entirely flat. This implies that every month has approximately 1/12th of the annual emissions.